AD-A039 897 TEXAS TECH UNIV LUBBOCK DEPT OF ELECTRICAL ENGINEERING F/G 9/5
PULSE POWER SYSTEMS EMPLOYING MAGNETIC ENERGY STORAGE.(U)
MAY 77 T F TROST N60921-76-C-0092
UNCLASSIFIED NL

1 OF 1
ADA039 897

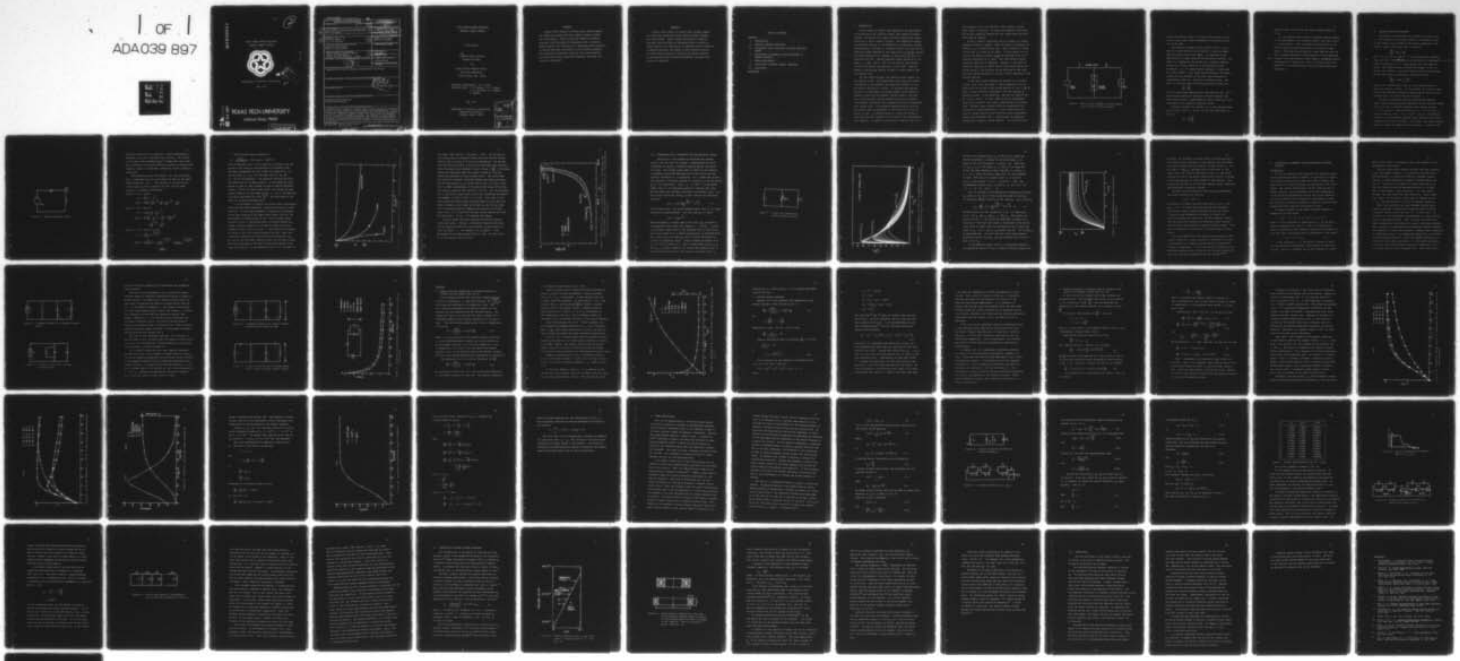

END

DATE FILMED
6-77

AD A039897

(2)

PULSE POWER SYSTEMS EMPLOYING MAGNETIC ENERGY STORAGE

DDC
MAY 25 1977
B

Department of Electrical Engineering

May, 1977

TEXAS TECH UNIVERSITY

Lubbock, Texas 79409

AD No.
DDC FILE COPY

DISTRIBUTION STATEMENT A
Approved for public release;
Distribution Unlimited

Unclassified

SECURITY CLASSIFICATION OF THIS PAGE (When Data Entered)

REPORT DOCUMENTATION PAGE

READ INSTRUCTIONS BEFORE COMPLETING FORM

1. REPORT NUMBER	2. GOVT ACCESSION NO.
3. RECIPIENT'S CATALOG NUMBER	rept.
4. TITLE (and Subtitle) Pulse Power Systems Employing Magnetic Energy Storage	5. TYPE OF REPORT & PERIOD COVERED Final 22 Dec 1975 to 21 April 1977
	6. PERFORMING ORG. REPORT NUMBER
7. AUTHOR(s) Thomas F. Trost	8. CONTRACT OR GRANT NUMBER(s) N60921-76-C-0092
9. PERFORMING ORGANIZATION NAME AND ADDRESS Texas Tech University Lubbock, Texas 79409	10. PROGRAM ELEMENT, PROJECT, TASK AREA & WORK UNIT NUMBERS
11. CONTROLLING OFFICE NAME AND ADDRESS Naval Surface Weapons Center White Oak Laboratory Silver Spring, Maryland 20910	12. REPORT DATE May 1977
	13. NUMBER OF PAGES 63
14. MONITORING AGENCY NAME & ADDRESS (if different from Controlling Office) 70p.	15. SECURITY CLASS. (of this report) Unclassified
	15a. DECLASSIFICATION/DOWNGRADING SCHEDULE

16. DISTRIBUTION STATEMENT (of this Report)

Approved for public release; distribution unlimited.

17. DISTRIBUTION STATEMENT (of the abstract entered in Block 20, if different from Report)

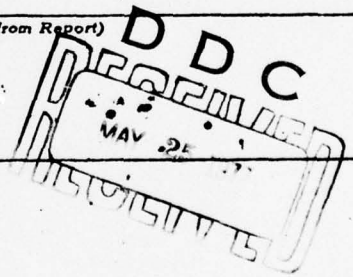

18. SUPPLEMENTARY NOTES

19. KEY WORDS (Continue on reverse side if necessary and identify by block number)

Inductive energy storage
Pulsed power systems

20. ABSTRACT (Continue on reverse side if necessary and identify by block number)

Several basic aspects of pulsed power systems supplying repetitive pulses and using inductive energy storage are investigated. These include the method of inductor charging, the efficiency of discharging with a resistive opening switch, the limitations of thermally driven resistors as opening switches, the design of pulse forming networks for time-varying resistive loads and the relative merits of voltage-fed versus current-fed networks, and some limitations on inductors.

DD FORM 1 JAN 73 1473 EDITION OF 1 NOV 65 IS OBSOLETE S/N 0102-014-6601

Unclassified

SECURITY CLASSIFICATION OF THIS PAGE (When Data Entered)

406820

PULSE POWER SYSTEMS EMPLOYING MAGNETIC ENERGY STORAGE

Final Report

Prepared under Contract

N60921-76-C-0092

for

Naval Surface Weapons Center

White Oak Laboratory

Silver Spring, MD. 20910

Principal Investigator: T. F. Trost

Research Staff: T. R. Burkes, P. D. Coleman, P. E. Garrison, M. O. Hagler, L. Masten

May, 1977

Department of Electrical Engineering

Texas Tech University

Lubbock, Texas 79409

SECTION for
NTIS White Section
DDC Buff Section
UNANNOUNCED
JUSTIFICATION
BY
DISTRIBUTION/AVAILABILITY CODES
Dist. AVAIL. and/or SPECIAL
A

ABSTRACT

Several basic aspects of pulsed power systems supplying repetitive pulses and using inductive energy storage are investigated. These include the method of inductor charging, the efficiency of discharging with a resistive opening switch, the limitations of thermally driven resistors as opening switches, the design of pulse forming networks for time-varying resistive loads and the relative merits of voltage-fed versus current-fed networks, and some limitations on inductors.

ABSTRACT

Several basic aspects of pulsed power systems supplying repetitive pulses and using inductive energy storage are investigated. These include the method of inductor charging, the efficiency of discharging with a resistive opening switch, the limitations of thermally driven resistors as opening switches, the design of pulse forming networks for time-varying resistive loads and the relative merits of voltage-fed versus current-fed networks, and some limitations on inductors.

TABLE OF CONTENTS

I. INTRODUCTION

In this report we examine some aspects of the performance of pulsers which use inductive rather than capacitive energy storage. We present the results of basic calculations, which should be of rather general interest. The impetus for employing inductive storage is the possibility of achieving a higher energy density, resulting in a smaller weight[1] and cost for the inductive system compared to the capacitive one of equal energy. The energy density in an inductor is given by $\frac{1}{2}\ \frac{B^2}{\mu_o}$ and in a capacitor by $\frac{1}{2}\ \varepsilon E^2$. Taking reasonable upper limits of B = 20 Tesla, $\varepsilon = 80\varepsilon_o$, and $E = 10^8$ V/m, we find for the inductor $1.6 \cdot 10^8$ J/m^3 and for the capacitor $2.8 \cdot 10^6$ J/m^3. Thus the magnetic field energy density is about 50 times greater than the electric one.

But one should consider the complete pulser system, not the inductor alone. The system must first cause the current to build up in the inductor, and then must transfer it into the load in the form of a pulse. In practice the greatest problem is in designing the opening switch, which opens the charging circuit so the inductor current flows to the load. Two or more switches opening sequentially may be required (for example, mechanical plus crossed-field tube or mechanical plus vacuum tube). The switching apparatus may be so large and complex that the advantage of the small size of the inductor is lost. In addition there is a basic difficulty in achieving efficient charging of an ordinary (not superconducting) inductor: in order to be efficient, charging has to be

done quickly; and so for storing a large energy, a large power input is required. In repetitive operation efficiency may be very important because the lost energy goes into heat which must be removed.

Figure 1 shows a simplified circuit diagram of a pulser employing inductive storage. When the source is charging the inductor, S_1 is closed and S_2 open. Then to deliver a pulse to the load, S_2 closes and S_1 opens. In this report we will consider the opening switch, S_1, to be represented by an increasing resistance as it opens. The load could be either primarily resistive or inductive. However, if the load is inductive, then one can show[2] that at most one-fourth of the energy stored in the inductor can be delivered to the load, with half being dissipated in S_1 and a fourth remaining in the storage inductor.

If the power source charges the inductor to a constant current level, then the power, P, being supplied to the inductor will be related to the stored energy, W_s, by $P = 2W_s \frac{R}{L}$. Thus, to ease the power requirement, the time constant $\frac{L}{R}$ should be large. If one wants W_s = 1MJ and the inductor has $\frac{L}{R}$ = 5 sec., then P = 0.4 MW. This is not an unreasonable power level, however, the current required may be extremely high. Possible power sources would use transformers and rectifiers or motor-generators. A very large working inductive storage system at the Arnold Air Force Development Center near Tullahoma, Tenn., uses Faraday (or homopolar) generators to charge a 100 MJ inductor. In this particular

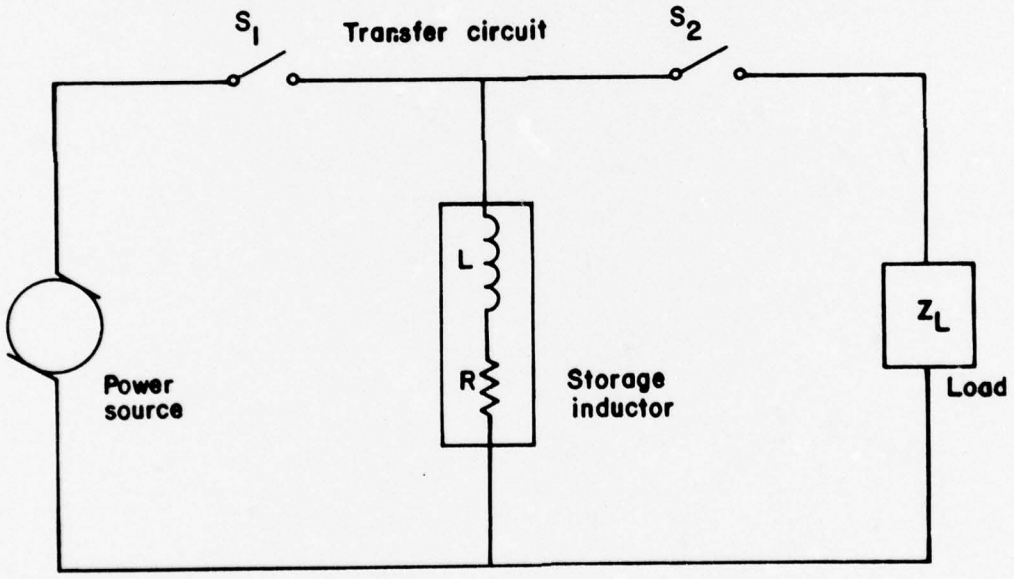

Figure 1. Basic circuit diagram of pulser system using inductive energy storage.

system the opening switch is in fact also the load, so one need not worry about power dissipated in the switch vis-a-vis in the load.

The essential purpose of the circuit in Fig. 1 is to deliver to the load for a brief period of time more power than the source alone could supply. An estimate of the amplification of power achieved is obtained as follows. The power, P_o, supplied by the source for a constant inductor current I_o is $I_o^2 R_c$, where R_c is the charging circuit resistance. R_c = R + power source resistance + resistance of S_1 when closed. If S_1 opens instantaneously, this exact current will be switched to the load, thus producing an instantaneous power $P_L = I_o^2 R_L$ (in a resistive load). The ratio of this load power to the source power is then just

$$\frac{P_L}{P_o} = \frac{R_L}{R_C} .$$

So for a large power amplification, one needs $R_C << R_L$. For a pulser using capacitive instead of inductive storage, the power amplification is approximately R_C/R_L, where R_C is the resistance of the capacitor charging circuit.

Finally, consider the voltage, V_o, of the charging power source fixed. Then $I_o = V_o/R_c$, and the peak load power is $I_o^2 R_L$ or

$$P_L = V_o^2 \frac{R_L}{R_C^2}$$

Thus the power delivered to the load is rather sensitive to R_c.

In the chapters that follow we consider several aspects of the performance of an inductive pulser, like that in Fig. 1, in more detail. Also a thermally driven switch for inductive energy storage applications is analyzed in some detail. The power conditioning for cases when one does not want a simple exponential output waveform is also described together with some physical limitations on inductive storage. The material in chapters 2,3, and 5 is largely taken from papers[3,4] in the Proceedings of the 1976 IEEE Pulsed Power Conference.

II. INDUCTOR CHARGING TECHNIQUES

We consider first charging an inductor for a short time, Δt. The increase in the energy stored in the magnetic field of the inductor ΔW_s, divided by the energy dissipated in the inductor series resistance, ΔW_D, is given by

$$\frac{\Delta W_s}{\Delta W_D} = \left(\frac{L}{R}\right) \frac{1}{i} \frac{\Delta i}{\Delta t}.$$

Now $\Delta i/\Delta t$ is like i/T, where T is the characteristic charging time; and $L/R = \tau$, the inductor time constant. So for good charging efficiency, i.e., large $\Delta W_s/\Delta W_D$, one must make τ/T large. This means charging quickly with respect to the inductor time constant. Leisurely charging would be inefficient. On the other hand, for charging a capacitor we have

$$\frac{\Delta W_s}{\Delta W_D} = 1/\left(RC \frac{1}{v_c} \frac{\Delta v_c}{\Delta t}\right),$$

where R is in series with C and v_c is the voltage across C. Here slow charging is best. In this regard, it is easy to show further that charging a capacitor quickly by the use of a step voltage source is at most only 50% efficient.

In order to determine inductor charging efficiencies under various charging-current waveforms, we have used the simple circuit of Fig. 2 with the following three voltage sources: 1. $v(t) = K_o u(t)$, a step of voltage K_o, 2. $v(t) = K_1 tu(t)$, a ramp of slope K_1, and 3. $v(t) = K_2 u(t) + K_3 i(t)$, the armature voltage of a self-excited, constant speed generator with linear feedback from field to armature. For source 3 the energy storage inductor is thus the generator field winding. In practice the

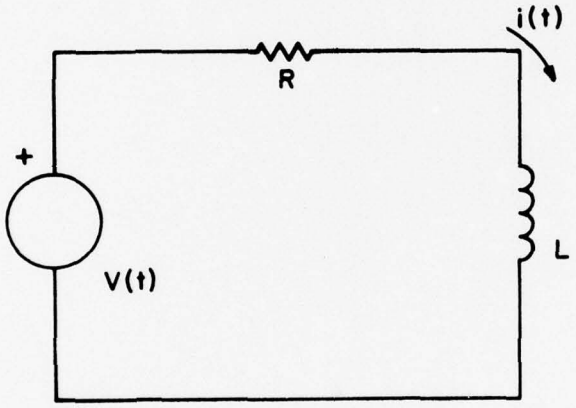

Figure 2. Inductor charging circuit.

generator might be a D.C. generator, either conventional or homopolar, or an A.C. generator and rectifier. The circuit is like that used by Robson *et al.*[5], except that their homopolar generator is not motor driven as current is drawn by the inductor, and so it slows down, converting inertial energy to electrical.

The equations giving the current, $i(t)$, and the energy, $W_D(t)$, dissipated in R are given below for each of the three charging sources. $\frac{L}{R} = \tau$. The current for the step source rises toward K_o/R as a function of time; for the other sources, it increases indefinitely.

Source 1: $v(t) = K_o u(t)$

$$i(t) = \frac{K_o}{R}\left(1 - e^{-\frac{t}{\tau}}\right)$$

$$W_D(t) = K_o^2\left(\frac{t}{R} + \frac{2L}{R^2}e^{-\frac{t}{\tau}} - \frac{2L}{R^2} - \frac{L}{2R^2}e^{-\frac{t}{\tau}} + \frac{L}{2R^2}\right)$$

Source 2: $v(t) = K_1 tu(t)$

$$i(t) = K_1\left(\frac{t}{R} - \frac{L}{R^2} + \frac{L}{R^2}e^{-\frac{t}{\tau}}\right)$$

$$W_D(t) = K_1^2\left(\frac{t^3}{3R} - \frac{L}{R^2}t^2 + \frac{L^2}{R^3}t - \frac{2L^2}{R^3}te^{-\frac{t}{\tau}} - \frac{L^3}{2R^4}e^{-\frac{2t}{\tau}} + \frac{L^3}{2R^4}\right)$$

Source 3: $v(t) = K_2 u(t) + K_3 i(t)$

$$i(t) = \frac{K_2}{R-K_3}\left(1-e^{\frac{(K_3-R)t}{L}}\right)$$

$$W_D(t) = R\left(\frac{K_2}{R-K_3}\right)^2\left(t + \frac{2L}{R-K_3}e^{\frac{(K_3-R)t}{L}} - \frac{L}{2(R-K_3)}e^{\frac{2(K_3-R)t}{L}} - \frac{3L}{2(R-K_3)}\right)$$

The efficiency during charging is

$$E_c = \frac{W_s(t)}{W_s(t)+W_D(t)} \text{ , where } W_s(t) = \tfrac{1}{2}Li^2(t).$$

This is plotted in Fig. 3 as a function of current, with the arrows on the curves in the direction of increasing time. The source parameters for this figure are fixed at $K_o = V_o$ for the step, $K_1 = V_o/\tau$ for the ramp, and $K_2 = 2V_o$ and $K_3 = 2R$ for the generator. The generator delivers the highest efficiency of the three sources. If the generator parameters, K_2 and K_3, were allowed to take on several different values, a family of curves would result, all having the same general shape as the one shown in Fig. 3. As $t \to \infty$ the generator efficiency approaches the value $\frac{K_3-R}{K_3}$. The efficiency of the other two sources approaches zero.

It is worthwhile to consider the source power requirements along with the other parameters, charging efficiency, current, and time. It also seems advisable to compare the performance of the three sources at the same current level, that is, the same amount of stored energy, $\frac{1}{2}\,Li^2$. Both of these things are done in Fig. 4, where peak power is plotted versus efficiency, and the parameters of all three sources are varied instead of being fixed as in Fig. 3. The inductor was allowed to charge up until the current reached $0.9\ V_o/R$. Thus, the curves were generated from different source parameters (K_o, K_1, and K_3) and different charging times, but the same current. The curve representing the step voltage source begins at the lower left with $K_o = V_o$ and charging time $t = 2.3\tau$ and ends at

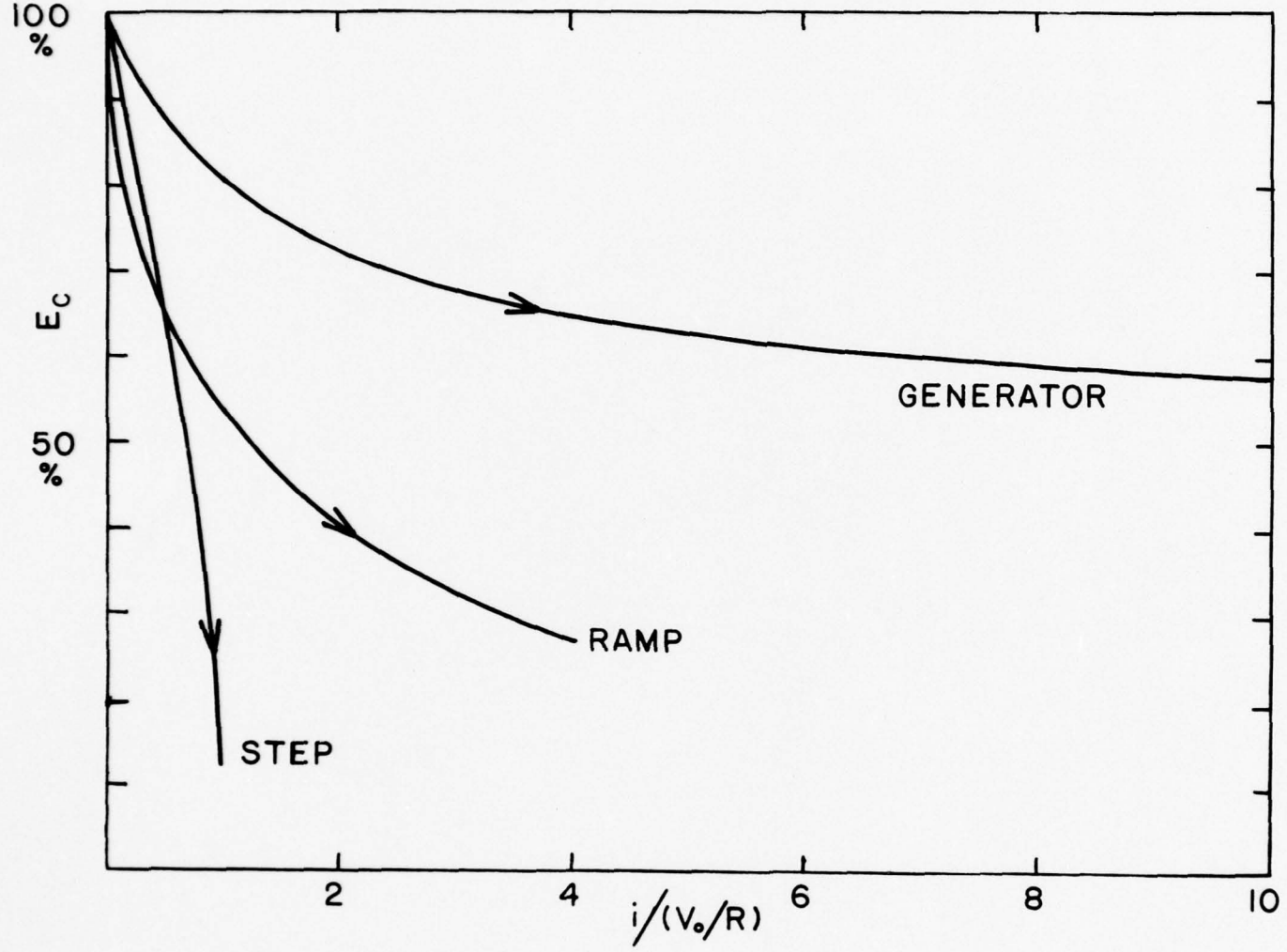

Figure 3. Charging efficiency vs. current. Time varies from 0 to 5 in direction of arrows.

the upper right with $K_o = 11V_o$ and $t = .092\tau$. So the size of the voltage step is increasing along the curve and the corresponding time to charge to $0.9\ V_o/R$ is decreasing. One can see that the efficiency goes up but so also does the power required. This high power occurs because a large voltage ($L\ \frac{di}{dt}$) is developed across the inductance when the current is made to rise very quickly by employing a large voltage source. The curve shows the nature of the basic trade-off between efficiency and power. For the ramp source, K_1 is varied from $0.3V_o/\tau$ to $7.0V_o/\tau$ from left to right corresponding to increasing the slope of the ramp and giving a charging time from 4.0τ to 0.56τ. For the generator, $K_2 = 0.5V_o$ and K_3 varies from 1.5R to 12R, increasing the amount of feedback, to give t from 1.3τ to 0.28τ. Note that for all three curves the source power plotted equals $0.9V_o/R$ times the source voltage, so one knows the voltage as well as the power. It is interesting that on comparing the sources at the same power level, it is found that the step source attains the highest efficiency. In Fig. 3 it attained the lowest.

Figure 4 shows that high charging efficiencies require high input powers. However, a reasonable charging efficiency can be obtained without too much increase in power above the level $P_o/(V_o^2/R) = 1$. For example, for $P_o/(V_o^2/R) = 2$ the efficiency of the step voltage source is 72%. For this value of P_o the charging time is 0.52τ.

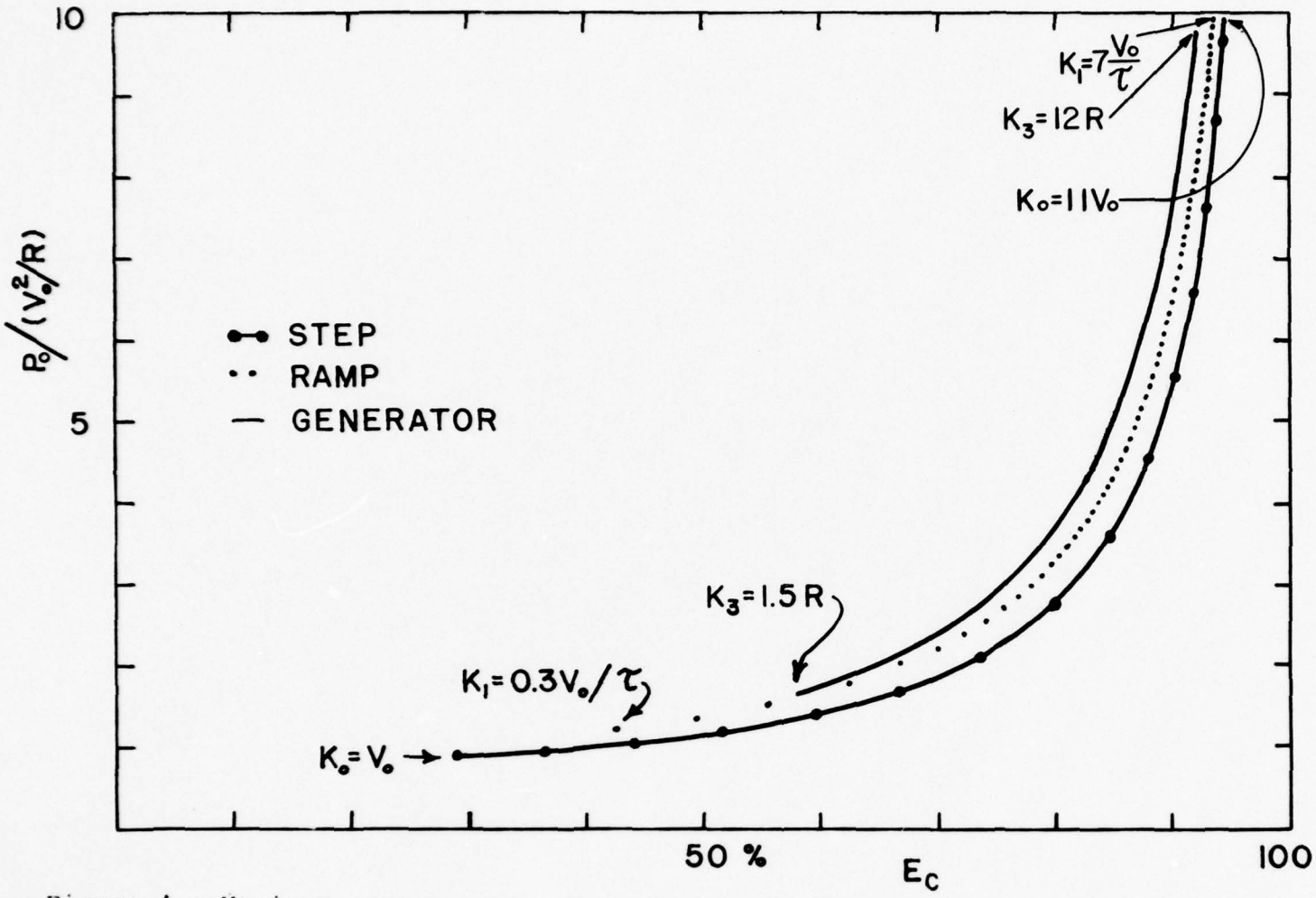

Figure 4. Maximum source power, P_o, vs. charging efficiency, E_c, for step, ramp, and generator sources. Inductor charged to a current 0.9 V_o/R. Source parameters, K_o, K_1, and K_3, varied as shown.

III. DISCHARGING WITH A RESISTIVE LOAD AND RESISTIVE SWITCH

Turning now to the problem of switching the inductor current into the load, we consider a simple parallel circuit consisting of inductor, resistive opening switch, and resistive load. The voltage source used to charge up the inductor is assumed to have been switched out of the circuit and the inductor resistance, R, is neglected. Fig. 5 shows the circuit. The inductor is initially charged to a current I_o, and the switch $R_s(t)$, is a dead short. $L/R_L = \tau_L$. At time t = 0 the switch opens; that is, its resistance starts to increase with time. We have taken the resistance variation to be linear; $R_s(t) = Kt$. The voltage across the load R_L is then given by the following equation:

$$v_L(t) = I_o K \left(1+\frac{K}{R_L}t\right)^{\frac{R_L}{K\tau_L}-1} te^{-\frac{t}{\tau_L}} . \qquad 3\text{-}1.$$

In the limit as $K\to\infty$, the switch becomes ideal, that is, it opens essentially instantaneously. For this case Eq. 3-1 gives

$$v_L(t) = I_o R_L e^{-\frac{t}{\tau_L}} ,$$

which represents a voltage jump to the value $I_o R_L$ followed by an exponential decay with time constant τ_L. Clearly, τ_L gives the intrinsic lower limit on the discharge time of the circuit. For finite values of K, a smooth voltage pulse is produced which has a peak value less than $I_o R_L$ and a trailing edge which is roughly an exponential decay. Figure 6 shows the pulses (from Eq. 3-1) for 19 values of K. The K values range from R_L/τ_L to 100 R_L/τ_L, and were chosen so as to make the "opening time" of the switch some fraction of the intrinsic discharge time τ_L.

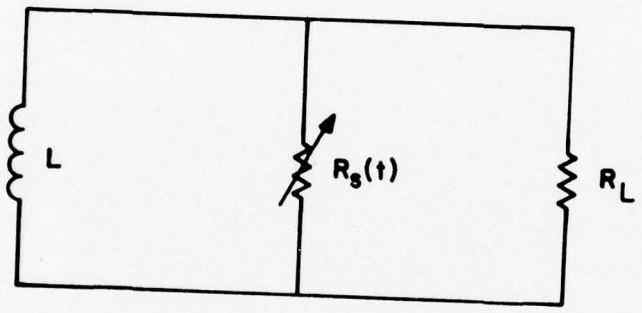

Figure 5. Circuit for transferring inductor energy to load.

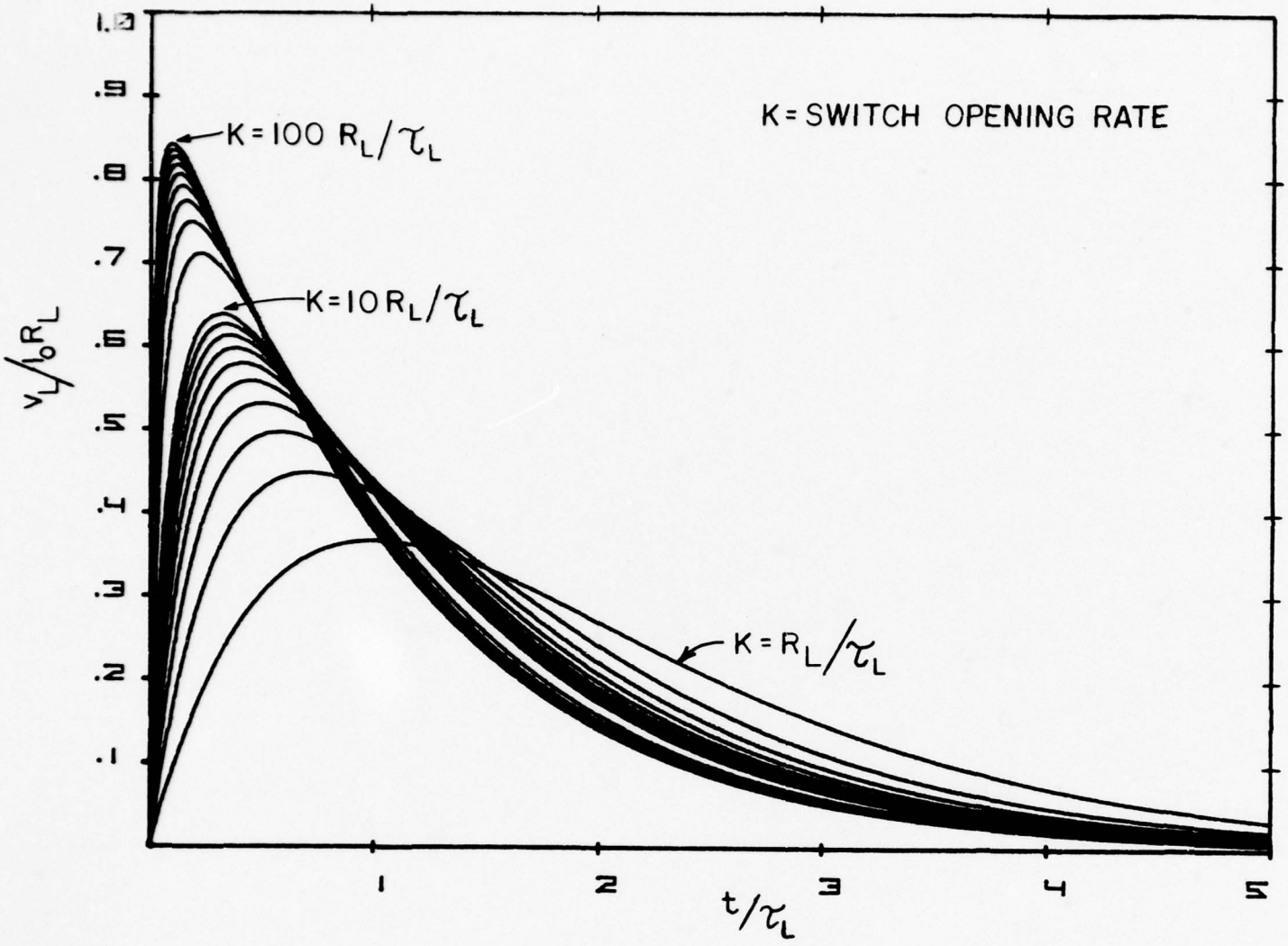

Figure 6. Load voltage, v_L, vs. time, t, for discharge of inductor in circuit of Fig. 4. $R_s(t) = Kt$. K varies from R_L/τ_L to 100 R_L/τ_L.

We define the opening time, T_o, as the time it takes the switch resistance to increase to the point where it is equal to the load resistance, or $R_s(T_o) = R_L$. Thus when $K = R_L/\tau_L$, T_o is just equal to τ_L, that is, it takes the switch one time constant to open; and when $K = 100\ R_L/\tau_L$, $T_o = .01\tau_L$, where the switch takes only .01 time constants to open. The list of K's used in Fig. 6, in units of R_L/τ_L, is as follows: 1,2,3,...,10,20,30,...,100. The corresponding values of T_o, in units of τ_L, are 1.00, .50, .33,..., .10, .05, .033,..., .01.

Also of interest is the switching or discharge efficiency, E_D, which is the ratio of the energy delivered to the load to the energy ($\frac{1}{2}LI_o^2$) initially in the inductor. E_D is given by

$$E_D = \frac{2K^2}{R_L L} \int_o^t (1+ \frac{K}{R_L}t)^{\frac{2R_L}{K\tau_L} -2} t^2 e^{-2\frac{t}{\tau_L}}\ dt. \qquad 3\text{-}2$$

We have carried out the integration in Eq. 3-2 numerically for $K = R_L/\tau_L$, $2R_L/\tau_L$, $3R_L/\tau_L$,...,$10R_L/\tau_L$. The results are plotted in Fig. 7. For any K the efficiency increases as a function of time since most power is dissipated in the switch right after it opens, when its resistance is still small compared to R_L. For $K = R_L/\tau_L$, E_D reaches only 50%. For $K=10R_L/\tau_L$, E_D approaches 80%. For this case the pulse length between half-power points is $0.84\tau_L$, and the risetime (10% to 90% of peak) is $0.15\tau_L$.

If the complete pulser circuit is considered instead of the simplified circuit of Fig. 5, nearly identical results are

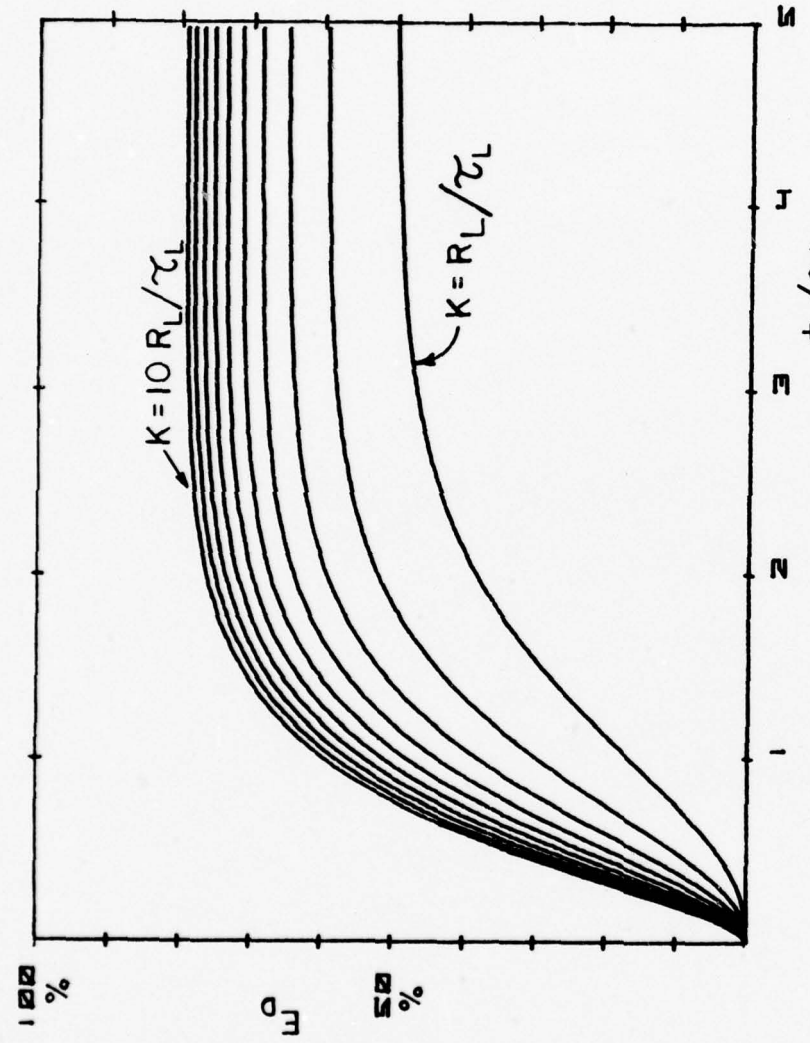

Figure 7. Discharge efficiency vs. time. K varies from R_L/τ_L to 10 R_L/τ_L.

obtained. We included a charging source in series with $R_s(t)$ and a small series resistance in the inductor and calculated an output voltage pulse very similar to those of Fig. 6. For the case $K = 10R_L/\tau_L$, the peak value of the pulse is .624 rather than .639, which is the value in Fig. 6. The slight reduction is due to the source, which tries to drive a current in the load opposite to that produced by the inductor. The calculation was done on our CDC 1604 computer using a modified IBM Runge-Kutta integration routine.

We have also calculated the load voltage produced when the switch resistance is given by

$$R_s(t) = e^{Kt} - 1$$

The results are nearly identical with those of Fig. 6 (for $R_s(t) = Kt$). For this reason and because the resistance variations of actual opening switches are not well known, it does not seem worthwhile to consider in detail any variation besides the linear one. We have, however, considered the resistance variation of thermally driven switches which may have applications to inductive energy storage. This work is described in some detail in a later chapter of this report.

It can be shown[6] that the opening switch studied in this chapter which has a linear increase in resistance with time, is equivalent to an inductive switch having an exponential increase in inductance. If the load itself is inductive, the switching problem is more difficult; and the basic results for this case have been discussed by various authors.[2,6-8]

IV. LIMITATIONS OF THERMALLY DRIVEN RESISTORS AS OPENING SWITCHES

Introduction

One of the simplest opening switches for inductive energy storage applications that is capable, in principle, of repetitive operation consists of a small wire that is heated, and hence driven to a high resistance, by the current to be interrupted. The current through such a device, which we call a thermal resistor, can be considered to be self-interrupting. In the following paragraphs we outline the initial phases of a study to determine the limitations in performance of thermal resistors as opening switches for inductive energy storage systems with both resistive and inductive loads.

A thermal resistor is one whose resistance depends on temperature as shown below,

$$v = v_o[1 + \alpha(T - T_o) + \beta(T - T_o)^2 + \gamma(T - T_o)^3]$$

where r is the resistance at temperature T, r_o is the resistance at temperature T_o, and α, β, and γ are coefficients that are properties of the resistive material.[9] For simplicity, only the linear relationship will be considered in this paper:

$$r = r_o[1 + \alpha(T - T_o)] \qquad 4\text{-}1.$$

If the resistance, r, of the thermal resistor is small, the resistor can be considered a closed switch in many applications. Then if r increases due to Joule heating to a point

where little current is allowed to pass, the resistor can be considered an open switch.

Several cases using a thermal resistor have been analyzed. First, the thermal resistor, r, is placed in parallel with a load resistance, r_L, which is driven by a constant current supply, I_o, which simulates an inductive storage device (see Fig. 8). Initially r is a small resistance less than r_L so that the voltage across the mechanical switch, S, is small when it first opens. Since initially $r < r_L$, the current through r will be larger than that through r_L. This current will cause r to rise until a final value is reached so that $r > r_L$. Now the majority of I_o will be passing through r_L.

Next, the possibility of using bistable thermal resistances as switches is studied for resistive loads driven by a constant current source (see Fig. 9). In this case, r is initially at a low resistance, corresponding to a closed switch, and in an equilibrium state. That is to say, the electrical power dissipated by Joule heating is equal to the power radiated. Since no energy is accumulated, the temperature remains constant and, therefore, so does the resistance. However, when a capacitor is discharged across r, for example, the equilibrium is disturbed and the resistance begins to rise until another equilibrium is achieved at some higher resistance. At this higher resistance, r cuts down the current passing through it significantly and the thermal switch can be considered open. Thus, this config-

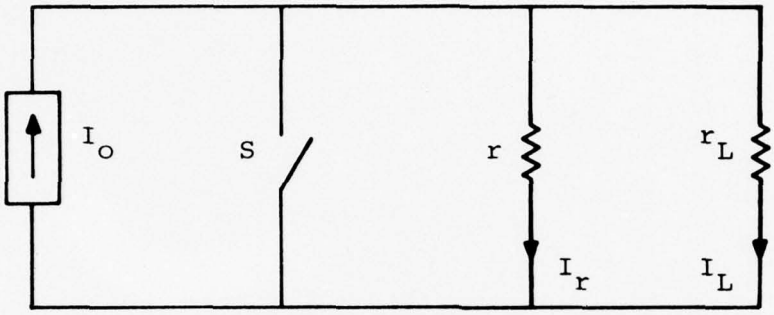

Figure 8. A thermal resistor as an opening transfer switch.

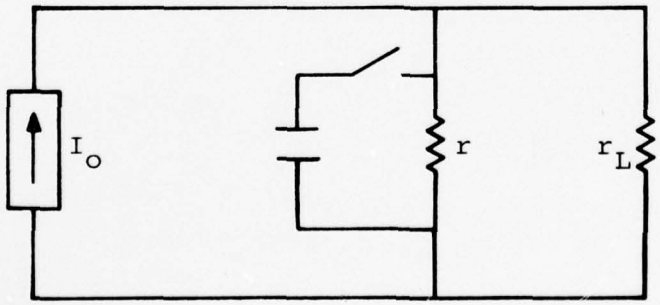

Figure 9. A thermal resistor as a bistable transfer switch.

uration offers the possibility of eliminating the mechanical opening switch.

The next circuit discussed is one in which the thermal resistor shunts an inductive load being driven by an inductive storage device. For simplicity a constant current source is used again to simulate the inductive storage device (see Fig. 10). If the thermal resistance, r, were absent, there would be a very high voltage across S due to the inductor, L, resisting a change in current when the mechanical switch S was opened. Therefore, if r is initially of low resistance and is placed in parallel with L, the initial voltage across S would be low enough to open it without arcing. Then as current passes through the thermal resistor, its resistance increases, forcing more and more current into L.

The last circuit considered (see Fig. 11) is similar to the one shown in Fig. 10 except that the constant current source I_o of Fig. 10 is replaced by a storage inductor L_o that has an initial current I_o flowing through it.

All circuits, except the last, were computer simulated. The circuit of Fig. 12 was chosen as a simple means of verifying certain modeling assumptions outlined below and the validity of the computer simulation code by comparing experimental and computed results. A tungsten light bulb was used for r, a constant voltage supply of 130 VDC for V_o, and a load resistance of 11 Ω for r_L. Computer and experimental results are shown in Fig. 12 for the current in the circuit vs time.

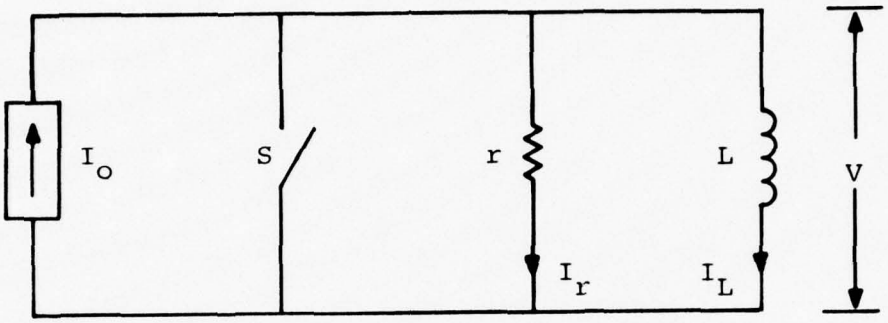

Figure 10. A thermal resistor as a current transfer switch with an inductive load.

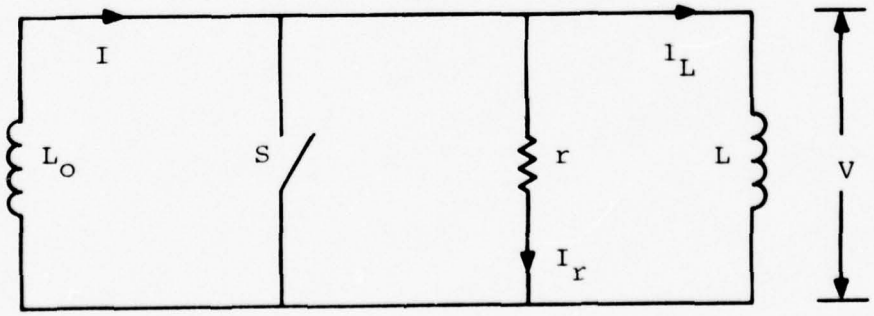

Figure 11. A simple inductive energy storage system with a thermal resistor transfer switch.

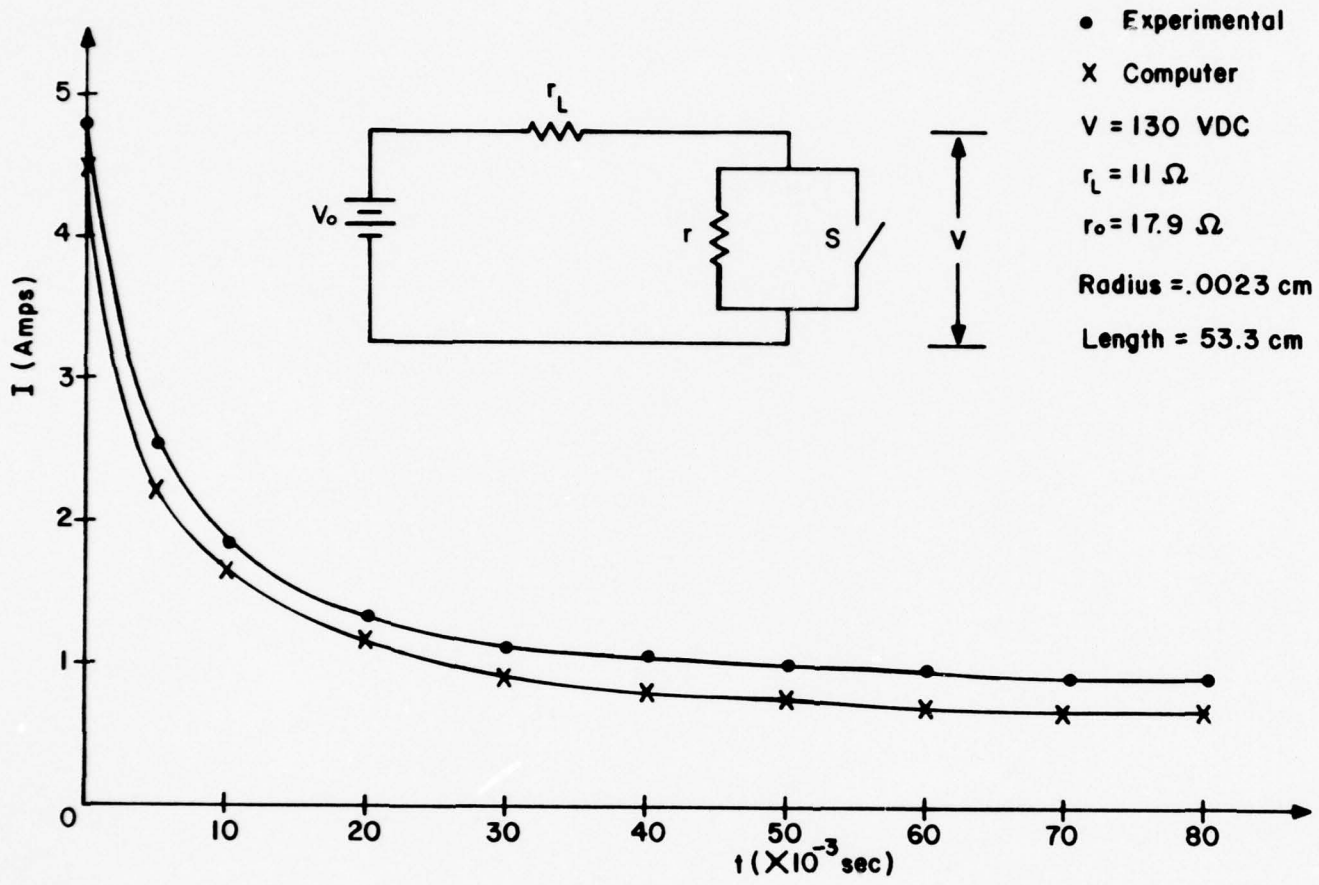

Figure 12. Comparison of experimental and computed values of I vs. t for the circuit shown.

Analysis

A. Thermal and load resistances in parallel driven by a constant current supply (see Fig. 8).

If the thermal resistor has a positive temperature coefficient of resistance, α, then Joule heating, $I_r^2 r = \frac{I_o^2 r_L^2 r}{(r+r_L)^2}$ will cause the resistance to increase with time. The total energy accumulated by the thermal resistor is that supplied by Joule heating minus the radiated energy. (We assume that the wire is long and thin and is placed in an evacuated chamber so that thermal conduction is not important). This accumulated energy causes a rise in temperature ΔT given by

$$\Delta T = \left[\frac{I_o^2 r_L^2 r}{(r+r_L)^2} - \varepsilon\sigma A_s T^4\right] \frac{\Delta t}{Mc} \qquad 4\text{-}2.$$

where ε is the emissivity of the thermal resistor material, σ is the Stefan-Boltzmann constant, A_s is the surface area of the thermal resistor, Δt is the time needed for a rise in temperature ΔT to occur, M is the mass of the thermal resistor, and c is the specific heat of the thermal resistor material, here assumed constant with temperature for simplicity.

Rearranging Eq. (4-2) we find an expression for $\frac{dT}{dt}$:

$$\frac{dT}{dt} = \left[\frac{I_o^2 r_L^2 r}{(r+r_L)^2} - \varepsilon\sigma A_s T^4\right] \frac{1}{Mc} \qquad 4\text{-}3.$$

By numerically solving Eq. (4-3), we can find the temperature of the thermal resistor for any time. The thermal resistance,

r, can then be found by use of Eq. (4-1).

Since one would like to reduce the current through the thermal resistor as much as possible, a large resistance ratio, $r^* = r/r_o$, is desirable. A high melting point and a large α make this possible. As seen from Eq. (4-3) a low specific heat, c, would increase $\frac{dT}{dt}$ and permit a quicker opening time for the thermal switch. Tungsten exhibits these qualities of a high r^* ($\tilde{\sim}$ 16 if r_o corresponds to room temperature) and low c, and is therefore chosen as the material for the thermal resistor in the initial studies.

Since the maximum value of $p^* \tilde{\sim} 16$ for tungsten, the best possible arrangement would be for $I_r = 4I_L$, initially, and $I_r = \frac{1}{4}I_L$ after Joule heating here I_r and I_L are the currents through the thermal and load resistances respectively.

From Eq. (4-3) it would appear that the thermal resistor should be designed with as little mass as possible to realize a large $\frac{dT}{dt}$. However, the thermal resistor must be massive enough to handle the initial current surge and the steady state current running through it so that melting does not occur.

Computer analyses were run for a cylindrical tungsten wire as the thermal resistor. A plot of r^* vs time is given in Fig. 13 for the following parameters: $I_o = 1820$ A and $V_L = 2\Omega$.

If the time needed to reach $r^* = 16$ is defined as the opening time of the switch, then for the above case, the opening time was approximately 0.9 sec. This was the best time

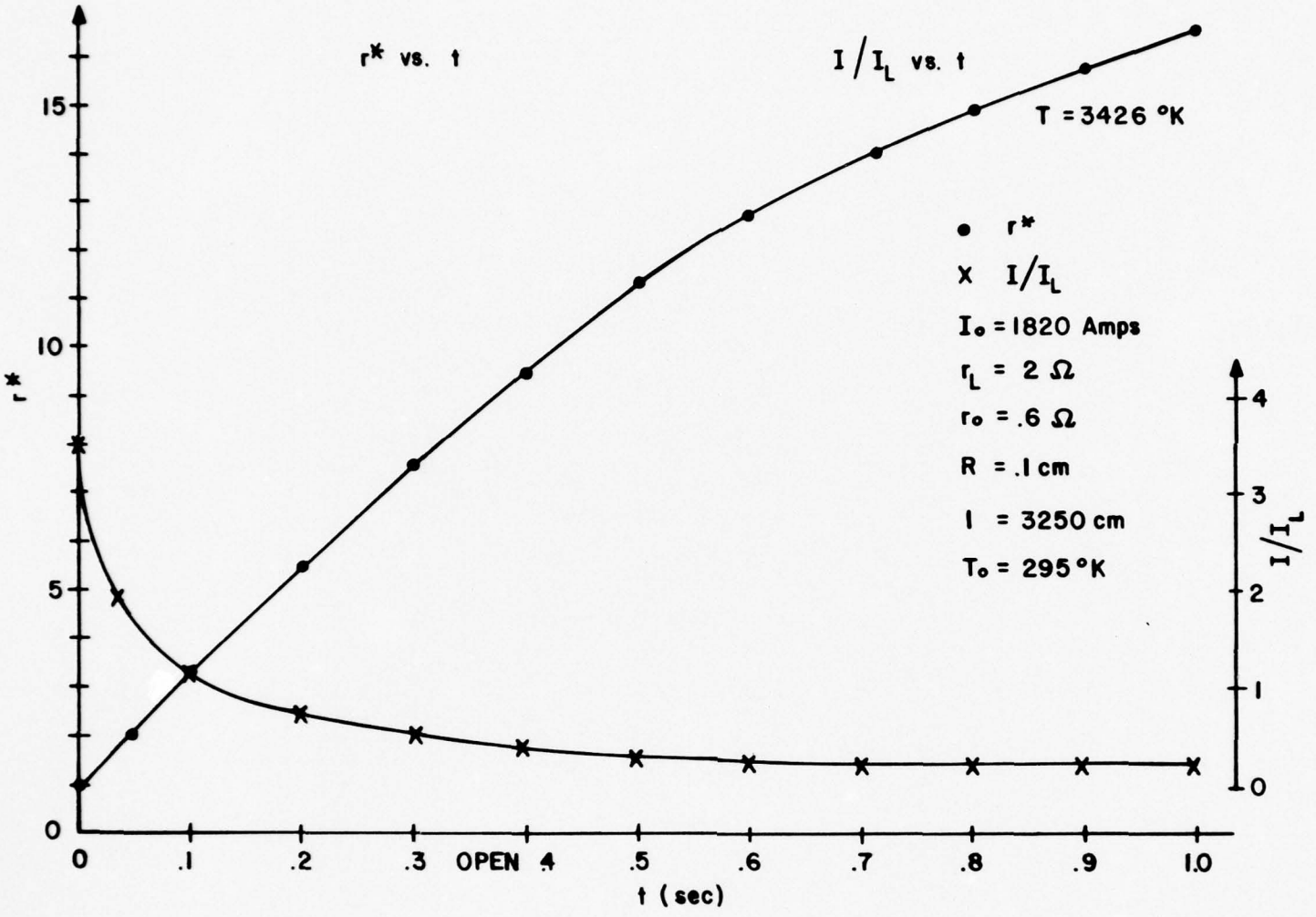

Figure 13. Optimized r^* vs. t for the circuit of Figure 8 with I_o = 1820A and $r_L = 2\Omega$.

achieved for I_o = 1820 A and V_L = 2 Ω by varying the dimensions of the wire.

B. Bistable thermal switches

Equation (4-3) also describes the temperature of the thermal resistor in the circuit of Fig. 9).

$$\frac{dT}{dt} = \left[\frac{I_o^2 r_L^2 r}{(r+r_L)^2} - \varepsilon\sigma A_s T^4\right] \frac{1}{Mc} \qquad 4\text{-}3.$$

Let

$$\delta = \frac{I_o^2 r_L^2}{Mc}, \quad \eta = \frac{\varepsilon\sigma A_s}{Mc}$$

Substituting δ and η into Eq. (4-3) we find

$$\frac{dT}{dt} = \frac{r\delta}{(r+r_L)^2} - \eta T^4$$

When an equilibrium state is achieved, $\frac{dT}{dt} = 0$ so that

$$\frac{r\delta}{(r+r_L)^2} = \eta T^4$$

or

$$\phi \equiv \frac{\delta}{\eta} = \frac{(r+r_L)^2}{r} T^4 \qquad 4\text{-}4.$$

If we multiply out the expression and substitute Eq. (4-1) for r we find an equation

$$F(T) = a_6 T^6 + a_5 T^5 + a_4 T^4 - a_1 T - a_o = 0$$

where

$$a_o = (1 - \alpha T_o) r_o \phi$$

$$a_1 = \alpha r_o \phi$$

$$a_4 = [r_L + r_o(1 - \alpha T_o)]^2$$

$$a_5 = 2\alpha r_o [r_L + r_o(1 - \alpha T_o)]$$

$$a_6 = (\alpha r_o)^2$$

Note that the T^2 and T^3 terms are missing from the polynomial F(T). We know, therefore, that at least one root has a positive real part. It is straightforward to see that the Nyquist plot[11] for F(T) encircles the origin exactly twice provided.

$$[r_L - r_o(1 - \alpha T_o)]^2 [r_L + r_o(1 - \alpha T_o)]^3 > (\alpha r_o)^4 \frac{\phi}{2}$$

4-11.

Since F(T) is a polynomial and hence has no poles, two encirclements means that there are two roots of F(T) with positive real parts. Because the coefficients $a_6, \ldots, a_o$ of F(T) are real, then its roots must be real or occur in complex conjugate pairs. Consequently, we must have either 1) a complex conjugate pair of roots with positive real parts or 2) two real roots with positive real parts. We argue from physical considerations that there is at least one positive real root of F - that is, we argue that there

is at least one temperature at which the system is at equilibrium. Thus, choice 1) above is ruled out. We therefore conclude that there are two positive real roots of F and hence two equilibrium temperatures. It is possible, of course, that the two roots are repeated roots, but this seems unlikely except for special combinations of parameter values. It is likely, therefore, that there are two distinct equilibrium temperatures for the circuit of Fig. 4-9 when Eq. 4-11 is satisfied.

If Eq. 4-11 is not satisfied, similar considerations lead to the conclusion that there may be only one positive real root plus a complex conjugate pair of roots with a positive real part. In this case, therefore, there may be only one equilibrium temperature. (In our application, only positive real roots of F have physical significance as equilibrium temperatures.)

In summary, Eq. 4-11 represents a sufficient condition for there to be two equilibrium temperatures, probably distinct. Questions that have not been addressed in this initial investigation include 1) the stability of the two supposed equilibria, 2) their temperature difference (and hence the difference in resistance r) for the two states, 3) the possibility of using resistors with more complicated dependence on T, and 4) the dynamics of the switching process. These matters should be studied, using numerical techniques, in a future investigation.

C. Thermal resistance in parallel with an inductive load driven by a constant current (see Fig. 10).

In this circuit two coupled first order differential equations arise. One describes the current in the inductor I_L, as a function of time, $\frac{dI_L}{dt}$, and one describes the temperature of the thermal resistor as a function of time, $\frac{dT}{dt}$.

To arrive at the equation for $\frac{dI_L}{dt}$, note that

$$I_o = I_r + I_L$$

$$V = I_r r = L \frac{dI_L}{dt}$$

where I_r is the current in the thermal resistor and V is the instantaneous voltage across r and L.

Manipulating these two equations, we find

$$\frac{dI_L}{dt} = \frac{r}{L} (I_o - I_L)$$

Now, substituting for r from Eq. 4-1, we obtain

$$\frac{dI_L}{dt} = \frac{r_o[1 + \alpha(T - T_o)](I_o - I_L)}{L} \qquad 4\text{-}5.$$

Now $\frac{dT}{dt}$ is found in the same way as it was in part A, but in this case the electrical power dissipated by Joule heating is $I_r^2 r = (I_o - I_L)^2 r_o[1 + \alpha(T-T_o)]$ so that Eq. 4-3 becomes

$$\frac{dT}{dt} = [(I_o - I_L)^2 r_o[1 + \alpha(T-T_o)] - \varepsilon\sigma A_s T^4] \frac{1}{Mc} \qquad 4\text{-}6.$$

For convenience the dimensionless variables x and y are introduced:

$$x = \frac{I_L}{I_o} \ , \ y = \frac{McT}{\frac{1}{2}LI_o^2}$$

where x represents the relative amount of current in L and y represents the ratio of the thermal resistor's energy at temperature T to the maximum energy stored in L's magnetic field.

Substituting x and y into Eqs. 4-5 and 4-6, we find

$$\frac{dx}{dt} = \frac{r_o}{L} \left[1 + \frac{\alpha \frac{1}{2}LI_o^2}{Mc} (y-y_o)\right](1-x) \qquad 4\text{-}7.$$

$$\frac{dy}{dt} = \frac{r_o}{L} \left\{2\left[1 + \frac{\alpha \frac{1}{2}LI_o^2}{Mc} (y-y_o)\right] - \frac{2\varepsilon\sigma A_s}{I_o^2 r_o}\left[\frac{\frac{1}{2}LI_o^2}{Mc}\right]^4 y^4\right\} \qquad 4\text{-}8.$$

Let

$$\tau = \frac{L}{r_o}, \ \alpha' = \frac{\alpha \frac{1}{2}LI_o^2}{M}, \ \beta = \frac{2\varepsilon\sigma A_s}{I_o^2 r_o} \left[\frac{\frac{1}{2}LI_o^2}{Mc}\right]^4$$

Now substituting τ, α', and β into Eqs. 4-7 and 4-8, we find

$$\frac{dx}{dt} = \frac{1}{\tau} \left[1 + \alpha'(y-y_o)\right](1-x) \qquad 4\text{-}9.$$

$$\frac{dy}{dt} = \frac{1}{\tau} \left\{2\left[1 + \alpha'(y-y_o)\right] (1-x)^2 - \beta y^4\right\} \qquad 4\text{-}10.$$

Here, τ represents a characteristic time of Eqs. 4-9 and 4-10. Since L is a parameter that cannot be varied once a particular system is chosen, r_o should be made large to make τ small and thus achieve a fast opening time. However, to avoid a large initial voltage across the mechanical switch S, r_o must not be made too large.

Computer runs varying α' and β were used to determine their effects on the opening time of the switch. Results of x and y vs normalized time = t/τ for various values of α' and β are given in Fig. 14. It was found that an increase in α' causes a quicker opening time. This should be expected since α' is a normalized temperature coefficient and the larger it is made, the faster r increases with time, which implies a quicker opening time. Although an increase in β caused a slightly slower opening time, it significantly cut down on the maximum value that y achieved, which is effectively the maximum temperature reached by the thermal resistor. Therefore, an increase in both α' and β is indicated for the best switch performance.

Note that α' and β depend on the physical properties of the material used for the thermal resistor (α, c, ε), the mass of the resistor (M), the geometry of the resistor (A_s), L, and I_o. The choice of tungsten as the thermal resistor would increase both α' and β because of its large temperature coefficient and low specific heat. An increase in I_o would cause α' and β to increase, although it would also cause a higher initial voltage across S and is therefore undesirable. As mentioned earlier, once a particular system is chosen, L may not be varied. A decrease in mass causes a larger α' and β, but if the mass is too small melting occurs.

Therefore, once the system, r_o, and the thermal resistor material have been picked only the geometry of the wire may be

Figure 14a. Normalized inductor current vs. normalized time for various values of system parameters.

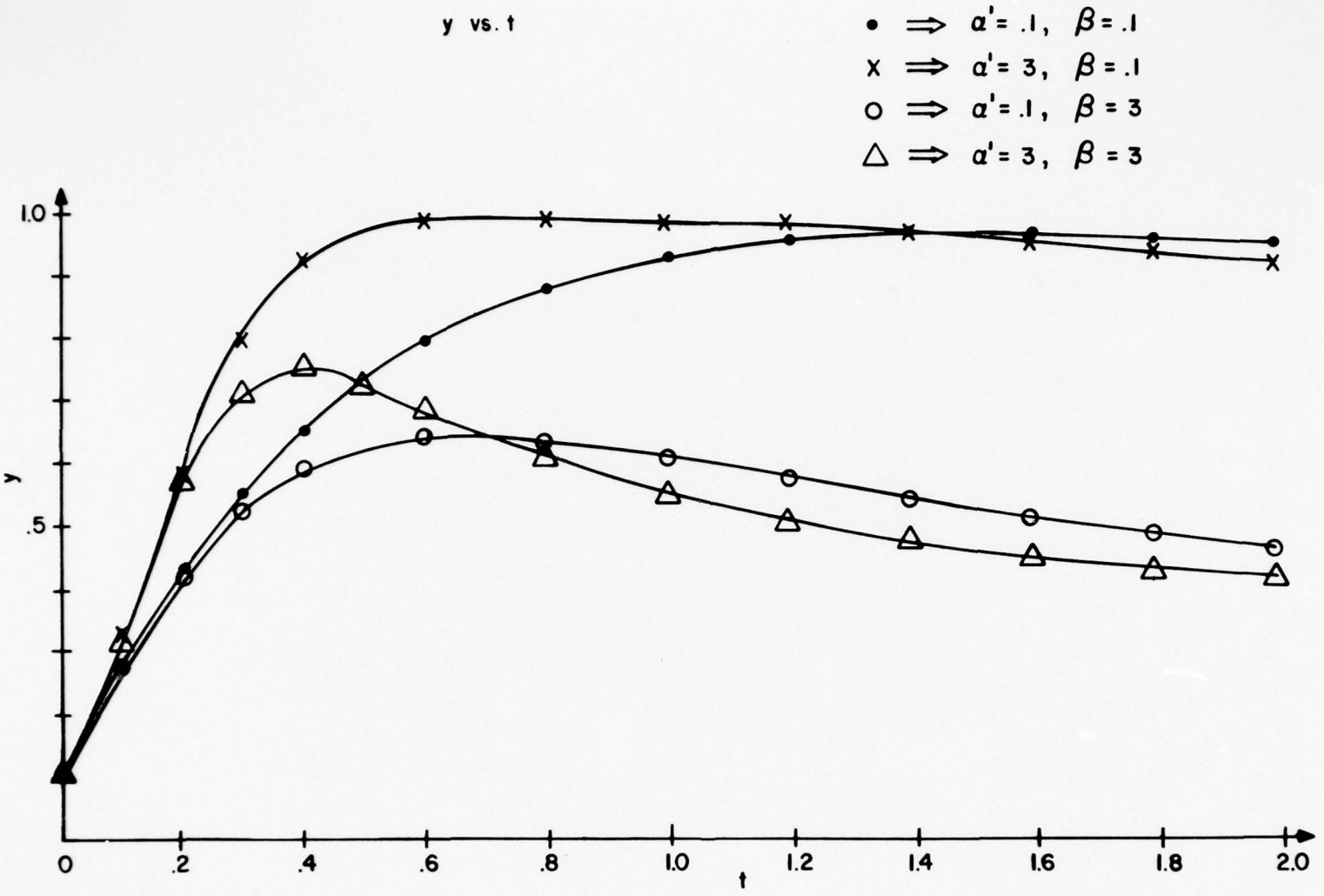

Figure 14b. Normalized temperature vs. time for various values of system parameters.

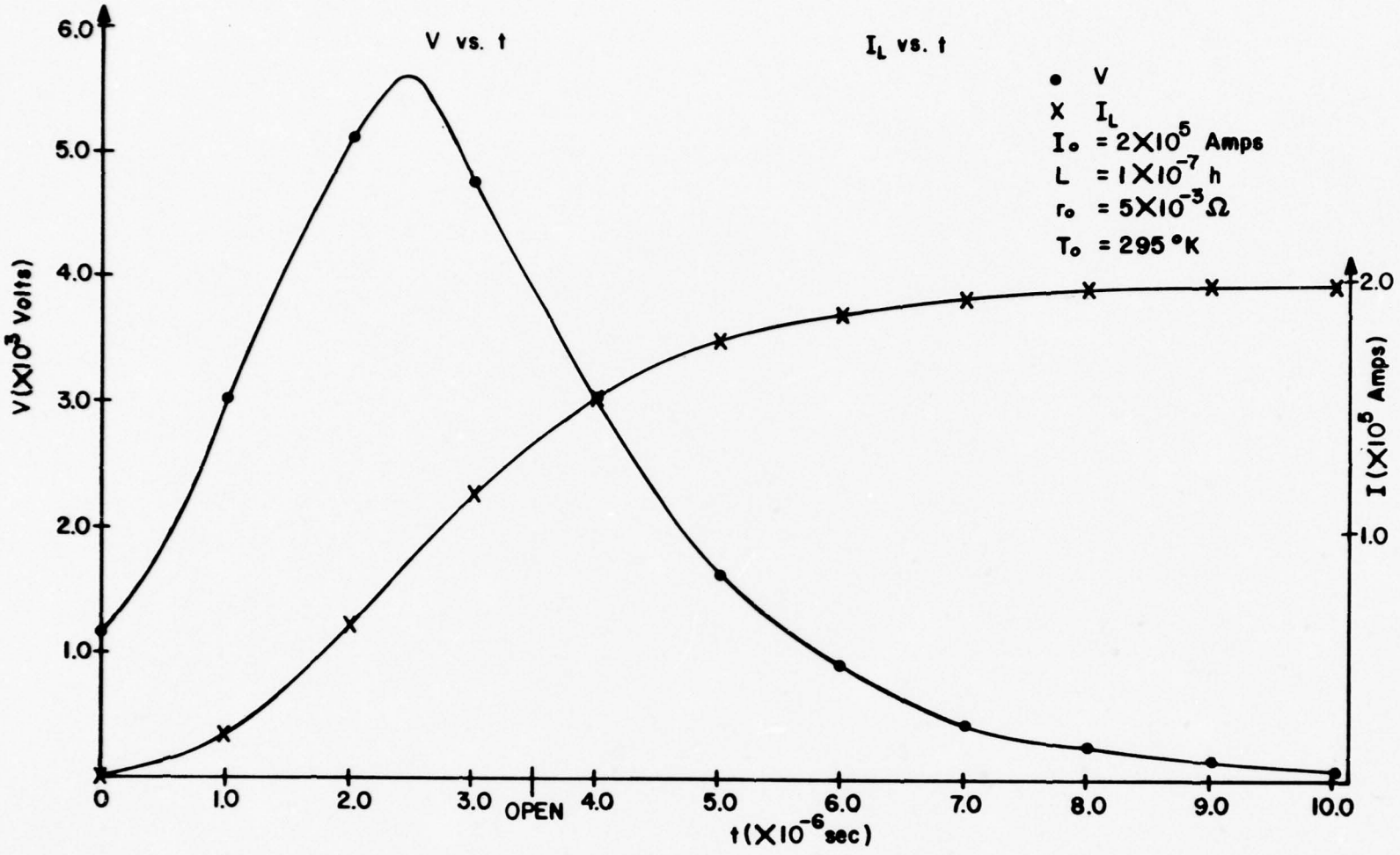

Figure 15a. Voltage vs. time for the circuit of Figure 10.

varied to decrease the opening time. The geometry is varied in such a way as to give the proper initial resistance with minimum mass to prevent melting of the thermal resistor.

Plots of V, I_L, and r vs. time are given in Fig. 15 for circuit parameter values of $I_o = 2 \times 10^5$ A, $L = 1 \times 10^{-7}$ h, and $r_o = 5 \times 10^3 \Omega$. An opening time, defined as the time for I_L to reach $(1 - 1/e)I_o$, of 3.5×10^{-6} sec. was obtained.

The final configuration we examined is shown in Fig. 11. Refering to this figure, we see that

$$I = I_r + I_L$$

and

$$V = L_o \frac{dI}{dt} = rI_r = L \frac{dI_L}{dt}$$

or

$$\frac{dI}{dt} = \frac{r}{L_o} I_r$$

$$\frac{dI_L}{dt} = \frac{r}{L} I_r$$

Proceeding as in previous cases, we find

$$\frac{dT}{dt} = \frac{1}{Mc}[I_r^2 r - \varepsilon\sigma A_s T^4]$$

or, using Eq. 4-1,

$$\frac{dT}{dt} = \frac{1}{Mc}[I_r^2 \, r_o[1 + \alpha(T-T_o)] - \varepsilon\sigma A_s T^4].$$

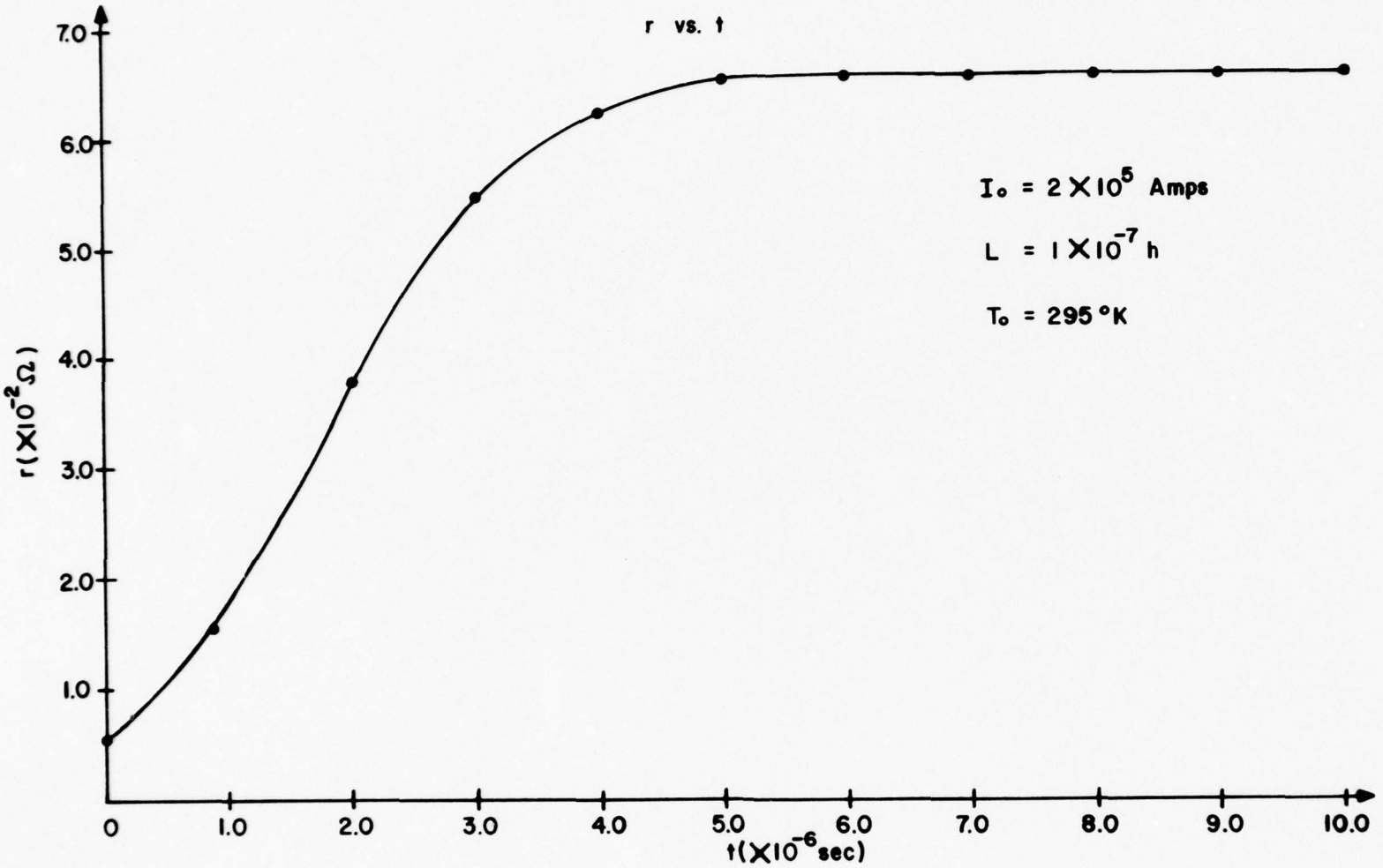

Figure 15b. Resistance vs. time for the circuit of Figure 10.

Let I_o be the initial current in L_o, $F_o = \frac{1}{2}L_o I_o^2$ be the initial energy in L_o and

$$x = \frac{I}{I_o} \ , \ y = \frac{I_L}{I_o} \ , \ z = \frac{I_r}{I_o}$$

$$w = \frac{McT}{E_o} = \frac{2Mc}{L_o I_o^2} T$$

Then

$$\frac{dx}{dt} = \frac{r_o}{L_o} [1 + \frac{\alpha F_o}{Mc} (w-w_o)]z$$

$$\frac{dy}{dt} = \frac{r_o}{L} [1 + \frac{\alpha E_o}{Mc} (w-w_o)]z$$

$$\frac{dw}{dt} = \frac{1}{E_o} \{I_o^2 z^2 r_o [1 + \frac{\alpha E_o}{Mc} (w-w_o)]$$

$$\frac{-2\varepsilon\sigma A_s}{L_o I_o^2} (\frac{E_o}{M_e})^4 w^4\}$$

Let $\tau_x = L_o/r_o$

$$\alpha' = \frac{\alpha E_o}{Mc}$$

$$\beta = \frac{2\varepsilon\sigma A_s}{I_o^2 r_o} (\frac{E_o}{Mc})^4$$

Since $z = x - y$, then

$$\frac{dz}{dt} = (\frac{1}{\tau_x} - \frac{1}{\tau_y}) [1 + \alpha'(w-w_o)]z$$

$$\frac{dw}{dt} = \frac{1}{\tau_x} \{2[1 + \alpha'(w-w_o)]z^2 - \beta z^4\}$$

These are state equations for the configuration of Fig. 11. We can approach choosing the various parameters by minimizing the function

$$J = \int_{t_o}^{tf} \{1 + z^2[1 + \alpha'(w-w_o)]\}\, dt$$

The first term in the integrand puts a premium on reducing the transition time, $t_f - t_o$. The integral of the second term represents the energy wasted in the resistor. The resulting optimization problem should be pursued to determine the maximum speed and minimum energy loss for this configuration.

V. POWER CONDITIONING

Most of the reported work in inductive energy storage utilizes the inductor to produce an exponentially decaying pulse (constant resistance load), or the inductor is used in an energy transfer scheme for magnetic confinement. However, many applications require a "square" pulse. A recent report[11] describes in detail the design and analysis of pulse forming networks (PFN's) in which the initial energy is stored in the inductors rather than the capacitors (current fed networks). This work utilizes a constant resistance load for the PFN. The treatment of current-fed PFN's is rather complete and will not be duplicated here.

It is highly likely that in the future pulsers will be required to drive more sophisticated loads which are nonlinear and/or time varying. PFN's for some nonlinear loads can be designed using classical techniques[12]. However, many gaseous discharge loads can be more conveniently described as time varying resistors. This kind of description for the load allows the design of a PFN which produces a constant current output pulse. Under the condition that the load is sufficiently well defined that it can be described as a time varying resistor, the methods of the well developed area of network synthesis can be applied. Guillemin derived a method of PFN design to produce constant voltage pulses into a constant resistive load. This method can be extended to design networks that will supply constant voltage pulses to time varying loads.[15] Basically, this

method assumes the short circuit current response of the network to be designed to be a periodic odd function of time. The positive half of this waveform is the required current to produce a constant voltage across the time varying load. By resolving the waveform into its Fourier components, a type C network can be obtained by comparing the magnitude and frequency of the individual Fourier components to the impulse response of a series L-C circuit. For the negative components, a separate network is designed which is placed in parallel with the load and is initially uncharged. An extension of this method may be made to produce constant current pulses into time varying loads. By employing the concept of duality, a current fed network may be derived. Voltage fed networks to produce constant current pulses are much more complex, but are more desirable because of switching considerations. In the following sections, the current fed network synthesis is developed and some of the requirements for voltage fed network design are defined.

The dual of a voltage-fed network is simply a current-fed network. An approach similar to Guillemin's Fourier series method would be to assume that a current fed network is "fired" into an open circuit. The resulting voltage can be described as an odd function of time and is required to be that voltage which would produce a constant current in the load. The Fourier series for the load voltage required to produce the constant current pulse I_L of width τ is obtained from

$$V_L(t) = R(t)\ I_L. \qquad 5\text{-}1.$$

$V_L(t)$ is the odd periodic function with a period of 2τ. The Fourier series would be

$$V_L(t) = \sum_{k=1}^{\infty} b_k \sin \frac{k\pi t}{\tau}, \qquad 5\text{-}2.$$

where

$$b_k = \frac{2}{\tau} \int_0^{\tau} V_L(t) \sin \frac{k\pi t}{\tau}\, dt,$$

or

$$b_k = \frac{2}{\tau} \int_0^{\tau} I_L R(t) \sin \frac{k\pi t}{\tau}\, dt. \qquad 5\text{-}3.$$

A modified Fourier coefficient can be defined as

$$d_k = \frac{b_k}{I_L}. \qquad 5\text{-}4.$$

In terms of these coefficients, the expression for the required voltage is

$$V_L(t) = \sum_{k} V_k(t), \qquad 5\text{-}5.$$

where

$$V_k = I_L d_k \sin \frac{k\pi t}{\tau}. \qquad 5\text{-}6.$$

An energy storage section which can be used to produce this component of $V_L(t)$ is shown in Fig. 16.

Using the initial conditions

$$V_k(0) = 0, \qquad 5\text{-}7a.$$

and

$$\left.\frac{dV_k}{dt}\right|_{t=0} = \frac{I_N - I_L}{C_k}, \qquad 5\text{-}7b.$$

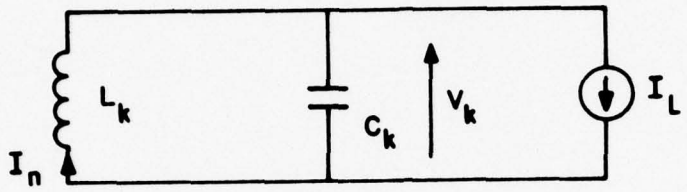

Figure 16. Section of current fed PFN with initial current I_N.

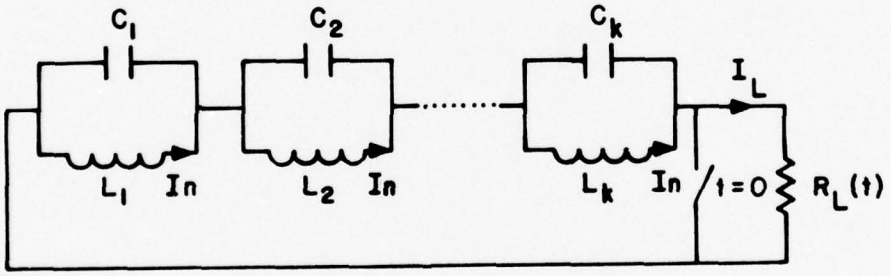

Figure 17. Six-section PFN for $R_L = \frac{1}{1 + t}$.

the solution of the differential equation describing the network of Fig. 16 is,

$$V_k = (I_N - I_L)\sqrt{\frac{L_k}{C_k}}\,\sin\left(\frac{t}{\sqrt{L_k C_k}}\right). \qquad 5\text{-}8.$$

Comparing this equation with Eq. 5-6, it is observed that

$$I_L d_k = (I_N - I_L)\sqrt{\frac{L_k}{C_k}}\,, \qquad 5\text{-}9a.$$

and

$$\frac{k\pi}{\tau} = \frac{1}{\sqrt{L_k C_k}}\,. \qquad 5\text{-}9b.$$

Solving Eq. 5-9a and 5-9b simultaneously gives

$$C_k = \frac{(I_N - I_L)\tau}{k\pi d_k I_L}\,, \qquad 5\text{-}10a.$$

and

$$L_k = \frac{I_L d_k \tau}{k\pi (I_N - I_L)}\,. \qquad 5\text{-}10b.$$

The Fourier coefficients, d_k, may be either positive or negative. Since the values for L_k and C_k must be positive, it is necessary to choose the initial condition, I_N, appropriately. That is, if

$$d_k > 0,$$

then

$$\frac{I_N}{I_L} > 1; \qquad 5\text{-}11.$$

but if $d_k < 0$,

then

$$\frac{I_N}{I_L} < 1. \qquad 5\text{-}12.$$

One possible choice for I_N is

$$I_N = 2I_L, \text{ if } d_k > 0; \qquad 5\text{-}13.$$

or

$$I_N = 0, \text{ if } d_k < 0. \qquad 5\text{-}14.$$

Although these are not the only choices for the initial conditions, they are convenient and they satisfy the conditions imposed by inequalities 5-11 and 5-12.

Therefore,

$$C_k = \frac{\tau}{k\pi |d_k|}, \qquad 5\text{-}15.$$

and

$$L_k = \frac{|d_k| \tau}{k\pi}, \qquad 5\text{-}16.$$

with $I_N = 2I_L$, if $d_k > 0$;

or $I_N = 0$, if $d_k < 0$.

As an example, suppose that $R_L(t)$ is given by

$$R_L(t) = \frac{1}{1 + t}, \quad 0 < t < \tau.$$

Then for Eqs. 5-3 and 5-4,

$$d_k = \frac{2}{\tau} \int_0^{\tau} \left(\frac{1}{1 + t}\right) \sin \frac{k\pi t}{\tau} \, dt.$$

The values for d_k, C_k, and L_k are tabulated in Table 1. The resulting network is shown in Fig. 17.

k	d_k	$C_k \mu F$	$L_k \mu H$
1	0.8675	0.3669	0.27613
2	0.1481	1.0754	0.02355
3	0.3133	0.3386	0.03324
4	0.0780	1.0227	0.00619
5	0.1897	0.3387	0.012
6	0.0527	1.0069	0.00279
7	0.1357	0.3350	0.00617
8	0.0397	1.0035	0.00158
9	0.1055	0.3352	0.00373
10	0.0318	1.0021	0.00101
11	0.0863	0.3353	0.00249
12	0.0267	0.9934	0.000709

Table 1. Fourier coefficients for $R_L(t) = \frac{1}{1+t}$.

The current response is shown in Fig. 18.

In this example the d_k values were all positive. If there had been negative terms, the network would take the form of Fig. 19. The inductors and capacitors corresponding to negative d_k are used for waveshaping purposes only. If these components are deleted, the resulting pulse is a very poor approximation to the desired "square" pulse.

To compare voltage-fed networks to current-fed networks is not always a straight forward matter. For complicated networks, an analysis of each design is required for definitive conclusions. The essential difference lies in the circuit configuration and the character of the switch (opening versus closing). In either case, both capacitors and inductors are required to produce a square pulse. Only for very particular and unusual loads can a square pulse be approximated using one element alone. Of

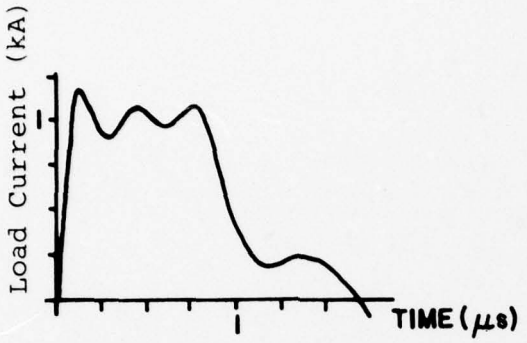

Figure 18. Current response for six-section PFN for $R_L = \frac{1}{1 + t}$.

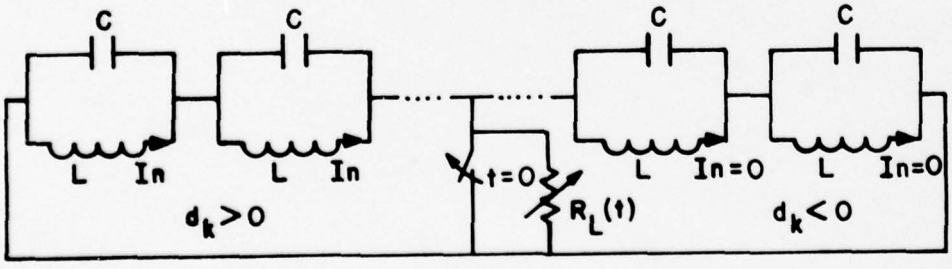

Figure 19. Network configuration for PFN with positive and negative d_K's.

course, the hard tube pulser performs this function by switch action for capacitive energy storage and can be made to perform the same function for inductive energy storage. However, this type of pulser design is a pulse shaping circuit depending on the switch function and beyond the intent of this chapter.

A few simple comparisons of the two PFN's can be gleaned from observations of response of a "Rayleigh line" (Fig. 20). This PFN is simply a lumped parameter approximation of a transmission line. Each L-C section is identical and the characteristic impedance, Z_o, and pulse width, τ, are:

$$Z_o = \sqrt{\frac{L}{C}} = \sqrt{\frac{\Sigma L_m}{\Sigma C_m}}$$

$$\tau = 2\sqrt{n^2 LC} \ .$$

For the voltage-fed case, all the energy is initially stored in the capacitors and at the same voltage. If the line is now "fired" into a matched load ($R_L = Z_o$), a pulse of duration τ and amplitude equal to half of the charge voltage will be delivered to the load. If, on the other hand, the line is shorted, a traveling wave of zero volts travels down the line toward the open end. At the instant

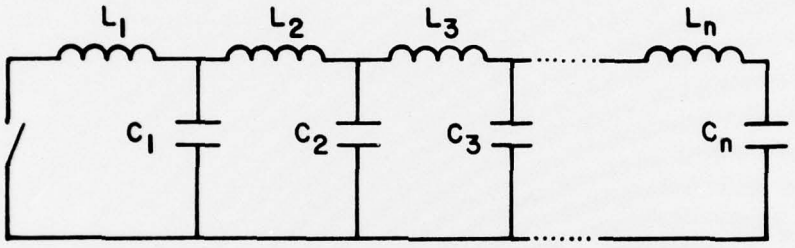

Figure 20. Circuit approximating a transmission line derived using Rayleigh's principle.

this wave arrives at the open end, the energy stored in capacitors will be zero and, as the network is lossless, all of the energy is now stored in the inductors. Thus, at this point the network can be viewed as current-fed rather than voltage-fed. If a load (R_o) were in parallel with the shorting switch and the switch "opened," a pulse identical to the voltage-fed case would be delivered. A few general conclusions can now be made comparing the weight/volume trade off's for the two cases assuming the same constant load, pulse duration, and energy. Also, repetitive operation is assumed.

Since reliable operation is required, a voltage-fed network must survive a faulted or shorted load. The analogous case for an "opened" load for the current fed case is not clear since a simple over voltage spark gap could be used for protection. In any event, under normal conditions (matched load), $\frac{1}{4}$ of the energy of the network will appear in either the capacitors or inductors depending on whether the network is current-fed or voltage-fed, respectively. Thus, the elements must be capable of sustaining this short time load and are, in this sense, equal. However, the duty cycle required of the respective elements is clearly not the same.

For current-fed networks, the charging current is twice the load current. As the network is "charged" over a considerably longer time than the pulse duration, considerable coil heating will occur. Also, the mechanical stress will be

applied over a longer time interval. Thus, it is clear that the inductors for the current-fed case must be cooled and be braced far more than for the voltage-fed case. Ordinarily, the inertia of the coils is sufficient for coil containment in voltage-fed networks. Also, coil cooling is minimal since load current only exists for the pulse duration. Definitive effects on coil weight/volume are determined by the specific application and, therefore, only these general conclusions concerning the coils can be made at this time. Suffice it to say the coils will be considerable heavier and more complicated by greatly expanded cooling requirements.

Assuming that the over voltage protection is provided for the current-fed network, more definitive conclusions can be made concerning the capacitors. If the maximum voltage allowed on the capacitors is 75% of that which would occur for an open circuited load, the maximum capacitive energy storage would be 56% of that required by a voltage-fed network. Thus, since capacitors scale approximately linearly with peak energy storage, the capacitors for a protected current-fed network would be approximately half the weight and volume of that for a voltage-fed network. All things considered, it is likely that the two networks will be comparable in weight and volume. Some advantage in volume is possible for current-fed networks because of the reduced peak voltage requirement. Again, the advantage would be determined by the specific application. For very high voltage applications, this advantage could make a considerable difference.

VI. LIMITATIONS ON ENERGY STORAGE INDUCTORS

One consideration in the design of inductors for high magnetic fields is the mechanical strength of the conductors. Figure 21[14] shows the magnetic pressure, $B^2/2\mu_o$, produced by a magnetic field B along with the yield points of several metals. For copper the yield point falls at about 30 Tesla, and beyond this, at around 80 Tesla, copper begins to melt.[2]

Two basic inductor designs are usually considered for inductive storage applications - the toroid and the solenoid. A coaxial inductor is also a possibility but gives only a fraction of a microhenry of inductance per meter of length.[15] The toroid has the advantage of good confinement of the magnetic field whereas the solenoid has poor confinement but can be optimized in the form of a Brooks coil[16] to yield the highest L/R of any inductor. For the Brooks coil one has[17]

$$\frac{L}{R} = \frac{.0255 \cdot 10^{-6}}{3\pi\rho(3\pi w)^{2/3}} \; f^{1/3} \; M^{2/3} \text{ sec.}, \qquad 6\text{-}1.$$

where ρ = resistivity of conductor in Ω cm, ω = density of conductor in gm/cm^3, f = fraction of winding occupied by conductor, and M = mass of conductor in gm. See Fig. 22 for the coil shape.

The field surrounding a Brooks coil is roughly that of a magnetic dipole, which has a $1/r^3$ variation with distance, r. To determine the value of L/R for an inductor with a somewhat more localized field, Marshall[20] has considered a mag-

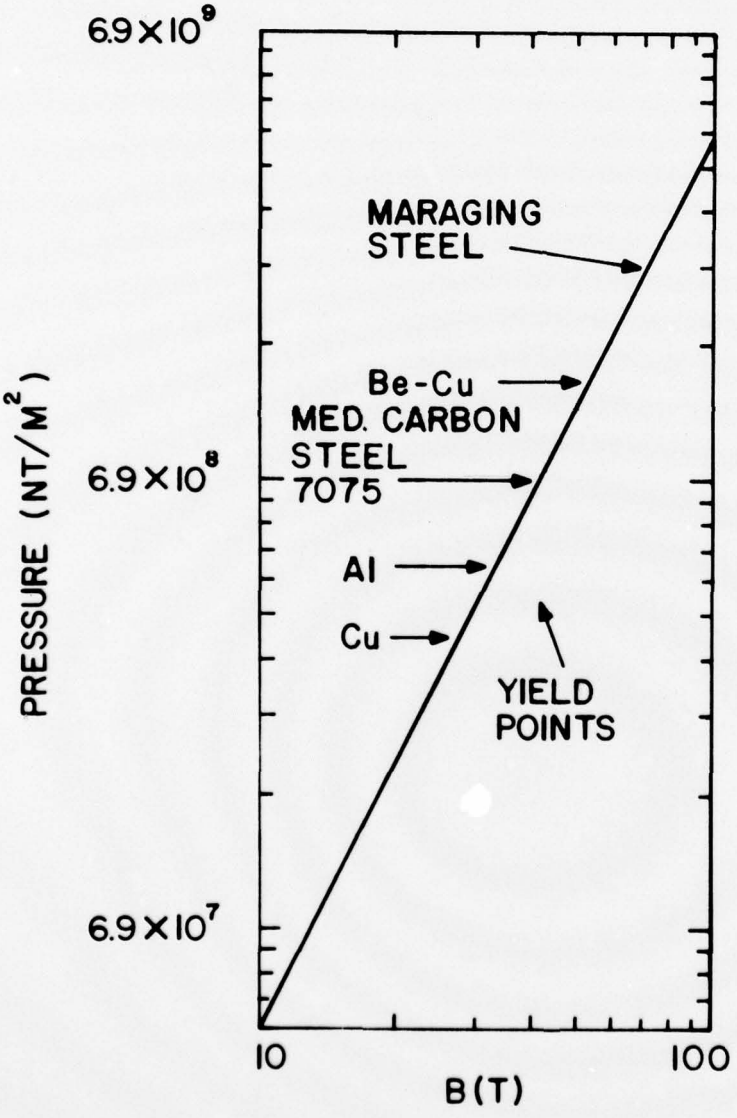

Figure 21. Magnetic pressure, $B^2/2\mu_o$, and yield point of various metals vs. B. From Ref. 14.

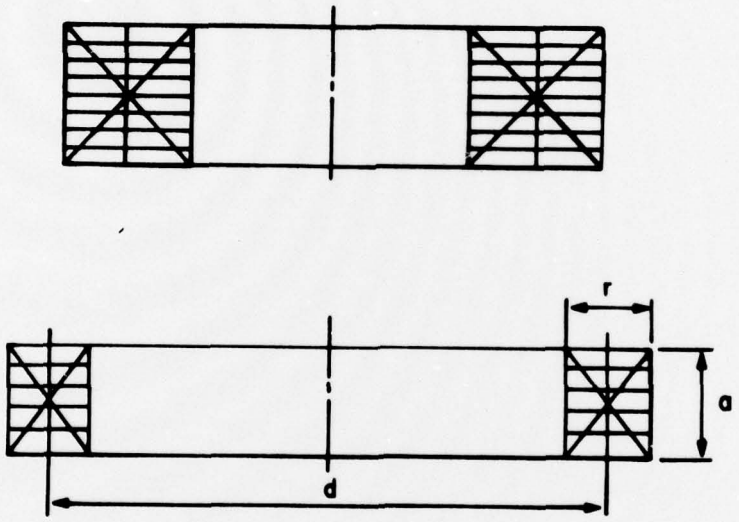

Figure 22. Cross section of Brooks coil (top) and of the solenoid (bottom) which is optimum for fast pulses where the field is trapped in the conductor. Both coils drawn to scale. From Ref. 19.

netic octupole consisting of a cluster of four rectangular solenoids. This gives a field that varies like $1/r^5$. Marshall finds that to obtain the same L/R for this arrangement as for a Brooks coil requires 3.65 times as much copper.

A magnetic field immersed in a good conductor obeys a diffusion equation. The diffusion time, T_d, is of order

$$T_d \sim \frac{\sigma \mu S^2}{4} ,$$

where σ is the electrical conductivity, μ the magnetic permeability, and S the characteristic dimension. For copper with a = .01 meter, $T_d \sim 2 \cdot 10^{-3}$ sec.

If an inductor is discharged into a load in a time much less than T_d, then essentially none of the magnetic field energy inside the wire is extracted. This case has been analyzed by Bystrov[18] for a solenoidal inductor. He finds that the ratios a/d = 0.2 and r/d = 0.15 are optimum instead of a/d = r/d = 0.33 as in the Brooks coil. See Fig. 22. Thus the geometry of the Brooks coil is optimum for slowly varying currents but not for rapidly varying ones.

An optimum toroid has also been determined[19] for the case where the flux is trapped in the conductor. Its weight is 5 times that of the optimum solenoid with the same power input and same energy output.

In addition to the problem of trapped flux in the conductors discussed above, another difficulty arises when trying to obtain short pulses from a storage inductor. The stray capacitance, C_s, of the inductor windings may cause the output voltage to ring instead of being a simple pulse. One way to think of

this is to consider increasing the load resistance, R_L, making the time constant, L/R_L, and thus the pulse length, shorter. This reduces the damping of the circuit until finally it becomes underdamped and rings.

The ringing frequency, $1/\sqrt{LC_s}$, determines the shortest time in which an output pulse can be obtained. But the stray capacitance also affects the output in another way. When the circuit is underdamped or even close to it, energy is transferred from the inductance to the stray capacitance as well as to the load. Thus the stray capacitance acts as an intermediate-storage capacitor bank; and if it cannot hold sufficient energy, then the energy output of the inductor is reduced. Schmitter[20] has calculated that if the capacitive energy storage density (of the inductor) is 1% of the inductive energy density and the circuit is critically damped, only about 6% of the maximum storable inductor energy can be delivered to the load.

Schmitter has also calculated the ringing frequency of a Brooks coil and found, for example, a minimum discharge time (for no capacitive effect) of 0.4 msec for a 1 MJ coil with current 10 kA, current density 10 kA/cm^2, and energy density 30 MJ/m^3. In order to reduce the discharge time, the energy density would probably have to be lowered, thus giving the coil less of an advantage in energy density over a capacitor bank.

Practical values of $\frac{L}{R}$ range up to perhaps 10 sec. Above this point the conductor mass becomes extremely large. See Eq. 6-1. For example, for a room temperature aluminum coil with f = 0.8 and a mass of 10 tons, $\frac{L}{R}$ = 4.78 sec. For 100 tons, $\frac{L}{R}$ = 22.4 sec.

Economics are of course important in the design of a storage inductor and of the whole system. The cost of a pulsed power supply using capacitive storage rises linearly with the stored energy while the cost when using inductive storage rises more gradually.[17] Thus there is a cross-over point lying between 0.1 and 10 MJ above which inductive storage is cheaper (for 100% discharge efficiency into resistive load). An interesting design of a 500 MJ inductive energy storage system is given in Appendix I of a design study for a Scyllac fusion test reactor by Thomassen.[21] A review of inductive, capacitive, and inertial energy storage systems for pulser applications has been given by Nasar and Woodson.[22]

VII. CONCLUSIONS

The work described in this report covers a spectrum of topics in the area of inductive energy storage. The following conclusions can be drawn:

The efficiency during inductor charging is limited by the increasing i^2R loss as the current is building up. The charging efficiency and input power requirement have been examined when three different voltage sources are used for charging: a simple voltage step, a ramp, and a self-excited generator connection which places the inductor in the generator field winding. For the generator connection the inductor current continues rising indefinitely and the charging efficiency levels off; for the other two sources, the efficiency falls toward zero. Although the efficiency with the generator can thus remain high, the power required is very high. On comparing the charging sources for a given stored energy and a given maximum input power, the simple step has the highest efficiency. Without excessive input power, efficiencies of about 70% are obtained.

Calculations of the basically exponential output pulse shapes in an inductive storage system with a resistive load and resistive opening switch have been carried out. They show that the peak value of the output pulse is about 37% of the value for an instantaneous switch when the switch

opening time equals one time constant (for the inductor and load) and 64% when the opening time is one-tenth the time constant. The division of stored energy between the load and the switch results in efficiencies of 50% and 80%, respectively, for the two opening times. The resistance rise of the switch with time was taken to be linear.

Thermally driven resistors show promise as simple, repetitive current transfer switches in inductive energy storage systems. A tungsten switch of this type can exhibit an open-to-closed resistance ratio of 16. Computer simulations show that opening times of microseconds are possible for certain parameter ranges, although typically the times are longer. Experimental confirmation of the calculation is shown for one simple case. Analysis indicates the possibility of operating thermally driven resistors as bistable switches with both open and closed equilibrium states. In principle, these switches can be easily triggered from their closed to their open state.

A method has been described for synthesizing a current-fed pulse forming network to deliver a constant current pulse into a time varying resistive load. An example of the method using a six-section network and the load $R_L(t) = \frac{1}{1 + t}$ gives a reasonably good pulse.

In a general comparison between voltage-fed and current-fed networks, it appears that the two will be roughly comparable in weight and volume, although the former will require larger capacitors and the latter larger inductors.

Inductive energy storage is more economical than capacitive storage when the stored energy is large. The minimum output pulse length depends on the stray capacitance of the inductor, and the maximum inductor $\frac{L}{R}$ time is limited by the mass of conductor that can be assembled.

REFERENCES

1. Alting-Mees, H. "Inductive Energy Storage Switching Technology for High Repetition Rate Lasers," Hughes Research Laboratories Rpt., Aug. 1973.

2. Knoepfel, H. Pulsed High Magnetic Fields (American Elsevier, New York, 1970).

3. Masten, L. and Burkes, T. R., "Constant Current PFN," IEEE International Pulsed Power Conference, p. III B3-1, Nov. 1976.

4. Trost, T. F., Garrison, P.E. and Burkes, T. R., "Pulse Power Systems Employing Inductive Energy Storage," IEEE International Pulse Power Conf., p. II D1-1, Nov. 1976.

5. Robson, A. E., et al, "An Inductive Energy Storage System Based on a Self-Excited Homopolar Generator," Proc. Sixth Symp. Eng. Probs. Fusion Res. (IEEE Pub. No. 75CH1097-5-NPS), p. 298, Nov. 1975.

6. Bailey, V., et al, "Advanced Concepts for Photon Sources-Volume 2: Fast Switching of Vacuum Magnetic Energy Stores," Physics International Co. Rpt. DNA 3680F-2, Aug. 1975.

7. Lee, T. H., Physics and Engineering of High Power Switching Devices (MIT Press, Cambridge, Mass, 1975).

8. Thomassen, K. I., "An Inductive Energy Storage System with Capacitive or Homopolar Transfer," LASL Rpt. LA-UR-73-1576, 1973.

9. Cheng, Dah Yu, Rev. Sci. Instrum. 40, 1153 (1969).

10. Wylie, C. R., Jr., Advanced Engineering Mathematics, (McGraw Hill, New York, 3rd Ed., 1960) 721-725.

11. Teno, J., et al, "Inductor Network Development for Aircraft High Power Supplies," Maxwell Laboratories, Inc., Rpt, 6 August 1976.

12. Glasoe, G. N. and Lebacqz, J. V., Pulse Generators (Dover, New York, 1948).

13. Ball, D. and Burkes, T. R., "PFN Design for Time Varying Load," IEEE Twelfth Modulator Symposium, p. 156, 1976.

14. Kristiansen, M. and Hagler, M. O., "Laser Heating of Magnetized Plasmas," Nuclear Fusion, Vol. 16, p. 999, 1976.

15. Inall, E. K. "A Proposal for the Construction and Operation of an Inductive Store for 20 Megajoules," U.K.A.E.A. Research Group Preprint CLM-P 225, Dec. 1969.

16. Grover, F. W., Inductance Calculations (Dover, New York, 1946).

17. Marshall, J., unpublished LASL report, 1965.

18. Bystrov, M. I., et al, "Characteristics of the Structure of Inductive Energy Storage Devices for Generating Short Pulses," Report on a Joint USSR-USA Seminar, Leningrad, NIIEFA, 1974.

19. Glukhikh, V. A., et al, "Pulsed Energy Sources Based on Inductive Accumulators," Preprint B-0299, Leningrad, 1976 (translation ERDA-tr-188).

20. Schmitter, K. H., "Dynamic Constraints on Inductive Energy Storage," Proc. Sixth Symp. Eng. Probs. Fusion Res., p. 296, Nov. 1975.

21. Thomassen, K. I., "Conceptual Design Study of a Scyllac Fusion Test Reactor," LASL Rpt. LA-6024, Jan. 1976.

22. Nasar, S. A. and Woodson, H. H., "Storage and Transfer of Energy for Pulsed Power Applications," Proc. Sixth Symp. Eng. Probs. Fusion Res., p. 316, Nov. 1975.